Geofísica Internacional 48 (1), 33-54 (2009)

El Chichón volcanic complex, Chiapas, México: Stages of evolution based on field mapping and $^{40}Ar/^{39}Ar$ geochronology

P. W. Layer[1], A. García-Palomo[2†], D. Jones[1], J. L. Macías[3*], J. L. Arce[2] and J. C. Mora[3]
[1]University of Alaska Fairbanks, Geophysical Institute, Fairbanks, AK, USA
[2] Instituto de Geología, Universidad Nacional Autónoma de México, Departamento de Geología Regional, Mexico City, Mexico
[3] Instituto de Geofísica, Universidad Nacional Autónoma de México, Departamento de Vulcanología, Mexico City, Mexico

Received: May 15, 2008; accepted: November 29, 2008

Resumen

Se presenta una nueva interpretación de la evolución del Volcán Chichón con base en fotogeología, trabajo de campo, química y fechamientos de rocas con el método de $^{40}Ar/^{39}Ar$. El Chichón forma parte de un complejo volcánico formado por cráteres y domos con un volumen total de ~26 km^3. El magmatismo en el complejo inició hace 370,000 años con la emisión de domos de lava actualmente sepultados por depósitos recientes. La actividad continuó con la formación de un complejo dómico andesítico (209,000-276,000 años) y flujos piroclásticos y lahares asociados. Este complejo dómico fue destruido por una erupción mayor que dejó un cráter de 1.5 km de diámetro conocido como Somma. La actividad continuó con la extrusión del Domo SW, hace 217,000 años en el borde suroeste del cráter Somma y con domos externos emitidos más allá del borde noroeste del mismo cráter hace 95,000 años. Dos bloques embebidos en los depósitos de la erupción de 1982 proporcionaron fechas de 44,000 y 29,000 años, lo que indica que el complejo estuvo activo durante el Pleistoceno. Durante el Holoceno la actividad magmática formó el cono de tobas Guayabal y un cono de tobas al interior del cráter Somma que fue reactivado en varias ocasiones, la última durante la erupción de 1982. Durante los últimos 8,000 años el complejo volcánico ha producido ~4 km^3 de material por lo que se estima una descarga de magma de 0.5 km^3/1000 años. Las rocas del complejo volcánico son andesitas potásico-alcalinas muy homogéneas.

Palabras clave: Fechamientos $^{40}Ar/^{39}Ar$, evolución, complejo volcánico, Chichón, México.

Abstract

A new interpretation of the evolution of El Chichón volcano is presented in this paper based on photogeology, fieldwork, $^{40}Ar/^{39}Ar$ dating and chemistry of juvenile products. El Chichón volcano belongs to a volcanic complex formed by craters and peripheral domes with a total estimated volume of ~26 km^3. Our data suggest that inception of magmatism began around 370 ka with the emission of lava domes buried by younger products. The activity continued with the formation of a large andesitic dome complex between 209 and 276 and associated block and ash flows and lahars. The dome complex was subsequently destroyed by a major eruption that left a 1.5-km wide Somma-type crater. The activity continued with the extrusion of the SW dome at 217 ka, that partially disrupted the southwestern Somma crater wall. Later on a series of dome extrusions occurred beyond the northwestern sector of the Somma crater at about 95 ka. Juvenile blocks found in 1982 products yielded ages of 44 and 29 ka attesting to heretofore unidentified late Pleistocene activity. The onset of Holocene activity occurred both outside the Somma crater with explosive eruptions that formed the Guayabal Tuff Cone and inside the Somma crater with the formation of a tuff cone that has been repeatedly reactivated during the Holocene, lastly during the 1982 eruption. All magmas produced during the past 370,000 years are K-alkaline andesites that exhibit minor variation in their chemical composition. An average discharge rate of 0.5 km^3/ka is calculated during the past 8,000 years (~4 km^3).

Key words: $^{40}Ar/^{39}Ar$ dating, evolution, volcanic complex, Chichón, México.

Introduction

El Chichón volcano (1100 m. above sea level) is one of the most active volcanoes in Mexico. It is located, 60 km southwest of Villahermosa, State of Tabasco, and 70 km north-northwest of Tuxtla Gutiérrez, State of Chiapas. Despite its proximity to these large capital cities the volcano is situated in a region with very difficult access. Up to the early twentieth century, El Chichón volcano was basically unknown to the volcanological community. The first description of El Chichón volcano was compiled following an episode of seismic unrest reported by inhabitants and described by Mülleried (1933). The fumarolic activity and the presence of a lake in the moat area prompted Mülleried to describe El Chichón as an active volcano. Almost fifty years later, Damon and Montesinos (1978) visited the volcano while doing field work in search of ore deposits in Chiapas. Because of its fumarolic activity these authors considered El Chichón to be the youngest volcano in the Chiapanecan Volcanic Arc (CVA), a NW-SE volcanic chain of Pliocene to Recent age (Fig. 1a). In addition, they obtained the first K-Ar date from andesite dome rocks of the moat area of the volcano, which yielded an age of 209 ± 19 ka. In 1980, the National Power Company (Comisión Federal de Electricidad) began evaluation of the El Chichón area for its geothermal energy possibilities (Canúl and Rocha, 1981). These authors presented the first general geological map of the volcano with a brief description of Jurassic to Tertiary sedimentary rocks and some volcanic units attesting to past eruptions. Between 1980 and 1981, coinciding with the geologic reconnaissance of Canúl and Rocha (1981), El Chichón seismic unrest began in the area increasing with time until early 1982 (Jimenez *et al*., 1998; Espíndola *et al*., 2002). Eruption began on March 28, 1982 and was followed by a catastrophic explosion on April 3 when pyroclastic surges and flows killed more than 2000 inhabitants. This event is the worst volcanic disaster to have occurred in Mexico in historical times. The 1982 event erupted 1.1 km^3 of magma (Carey and Sigurdsson, 1986) of trachyandesitic composition (56 wt. % SiO_2; Luhr *et al*., 1984) through Plinian columns higher than 27 km that injected ash into the stratosphere (Luhr 1991; Rampino and Self 1984). The juvenile products of the magma contain anhydrite, a mineral that had never been reported as a primary mineral in magmas (Luhr *et al*., 1984; Rye *et al*., 1984). All of these features led several specialists to the study of the crater lake (Casadevall *et al*., 1984), the pyroclastic deposits (Tilling *et al*., 1984; Sigurdsson *et al*., 1984; Rose *et al*., 1984; Sigurdsson *et al*., 1987), the ash and plume dispersion (Varekamp *et al*., 1984; Carey and Sigurdsson, 1986), the sulphur content of the magma (Devine *et al*., 1984; Carroll and Rutherford, 1987), and the petrology of the products (Luhr *et al*., 1984).

The pyroclastic density currents produced by the 1982 eruption stripped the vegetation cover exposing old pyroclastic deposits and allowed for the study of past volcanic events with the aid of radiocarbon and K-Ar geochronology. Duffield *et al*. (1984) dated an andesite dome rock from the eastern flank of the Somma crater at 276 ± 6 ka (K-Ar) and a thick widespread pyroclastic flow at 1250 yr BP (^{14}C). Tilling *et al*. (1984) published ^{14}C ages for other eruptions dated at 600 and 1750 yr BP. Macías (1994) reported two other events at 900 and 1400 yr BP. Espíndola *et al*. (2000) summarized the Holocene stratigraphy of El Chichón describing at least 11 deposits related to the same number of eruptions at 550, 900, 1250, 1400, 1700, 1800, 2000, 2400, 3100, 3700 and 7500 yr BP. The oldest volcanic rock in the area is the early Pleistocene (1.1 Ma) Chapultenango basalt erupted 10 km to the east of El Chichón (García-Palomo *et al*., 2004).

Despite the background provided by the ^{14}C and K-Ar geochronology, very little work has been done to constrain the Pre-Holocene history of El Chichón. In fact, the study of features such as the peripheral domes has been neglected except for some petrographic and chemical studies (e.g., Rose *et al*., 1984; McGee *et al*., 1987; Tepley *et al*., 2000). Therefore, several pressing questions need to be answered. For instance: When did andesitic volcanism begin in the area? How has magmatism evolved through time? What is the extent (spatially and volumetrically) of pre-Holocene magmatism?

The aim of this paper is to present preliminary results that constrain the longevity and evolution of El Chichón volcano by integrating field mapping, a photogeological map, digital elevation models (DEM), geochemistry and $^{40}Ar/^{39}Ar$ geochronology. With this information we present a preliminary model of the volcano as part of a volcanic complex composed of several structures.

Tectonic setting

The origin of El Chichón volcano has been related to the subduction of the Cocos plate beneath the North American plate at the Middle American Trench (Luhr *et al*., 1984; García-Palomo *et al*., 2004) (Fig. 1a). This ongoing subduction process is occurring at an average convergence rate of 66 mm/yr in a northeast direction (Pardo and Suárez, 1995). The projected slab is dipping at an angle of 40° and has an approximate thickness of 39 ± 4 km (Rebollar *et al*., 1999). This geometry sets El Chichón, which is at 400 km from the trench to about 300 km above the subducted slab under Chiapas (García-Palomo *et al*., 2006). The origin of El Chichón K-alkaline magmas are probably derived from the partial melting of the slab (Luhr *et al*., 1984; Rye *et al*., 1984; Luhr and Logan, 2002), which likely interacted in different proportions with the

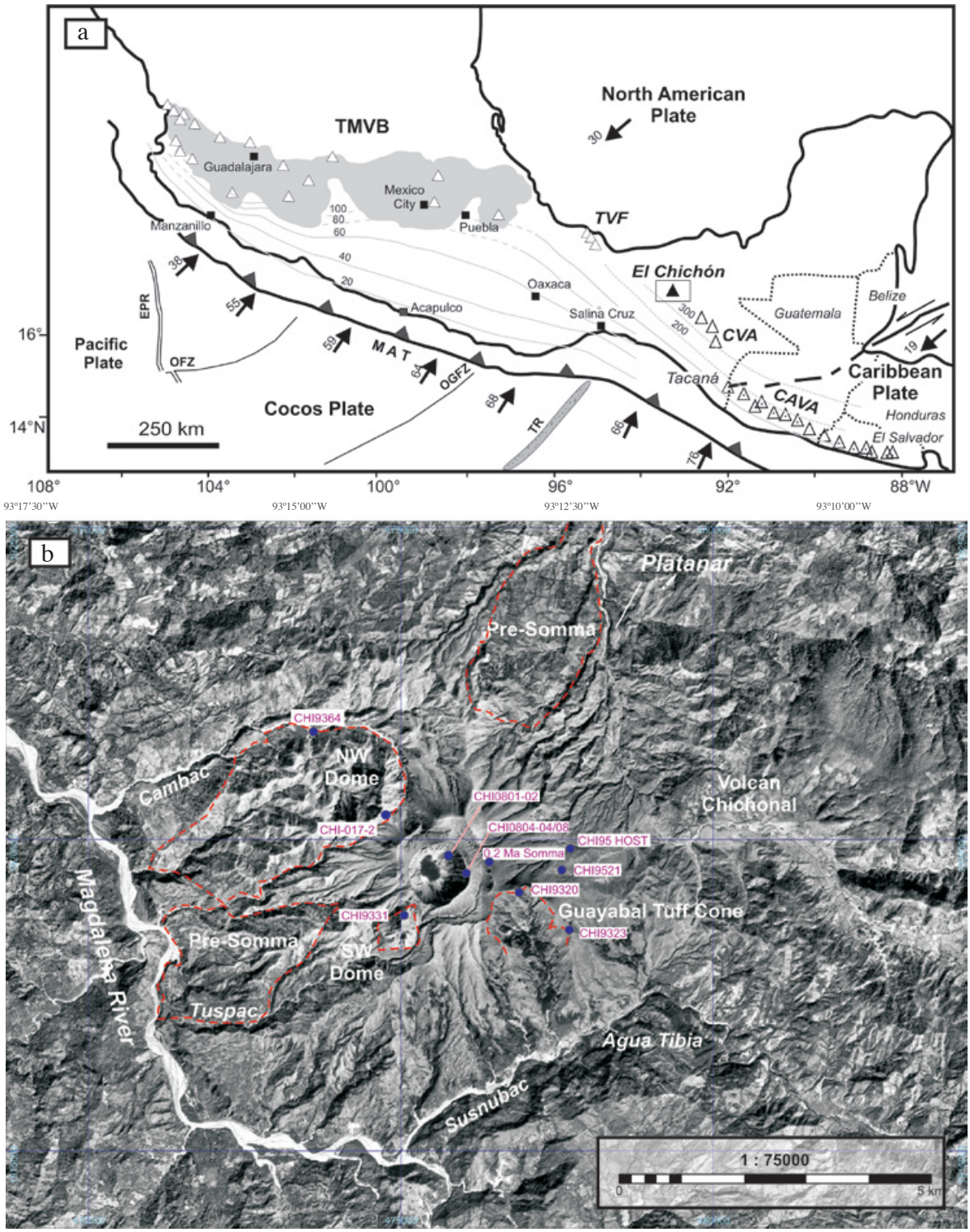

Fig. 1. a) Tectonic setting of El Chichón volcano in southern Mexico after García-Palomo *et al*. (2004). Abbreviations are: TMVB= Trans-Mexican Volcanic Belt, TVF= Los Tuxtlas Volcanic Field. CAVA= Central American Volcanic Arc, CVA= Chiapanecan Volcanic Arc, RFZ = Rivera Fracture Zone, EPR = East Pacific Rise, OFZ = Orozco Fracture Zone, MAT = Middle American Trench, OGFZ = O'Gorman Fracture Zone, and TR = Tehuantepec Ridge. The solid lines are isodepth contour lines from Pardo and Suarez (1995) and Rebollar *et al*. (1999), and dashed lines indicate extrapolation of data due to the lack of hypocenters. Arrows are relative convergence rates of the different plates in mm/yr. b) Location of samples used for Ar-Ar dating (see Table 1 for details).

mantle wedge (Taran *et al.*, 1998), and the crust (Tepley *et al.*, 2000; Espíndola *et al.*, 2000; García-Palomo *et al.*, 2004). However, Nixon (1982) has proposed an alternate hypothesis for the origin of El Chichón volcano and its K-alkaline volcanism as being related to extensional tectonics in southern Mexico associated with the triple junction between the North American, Caribbean, and Cocos plates.

Superimposed to the subduction tectonic setting there is a regional system of sinistral strike-slip faults called the Transcurrent Fault Province (Meneses-Rocha, 1991). This province has been divided into three major areas: Eastern, Central, and Western. El Chichón lies within the Central area, which is characterized by strike-slip faults with northwest trend (Meneses-Rocha, 1991).

Local geology

Locally El Chichón has been built upon a sedimentary substrate composed of Late Jurassic evaporites, Middle Cretaceous limestones, and Middle Miocene claystones and sandstones (Canul and Rocha, 1981; Canul *et al.*, 1983; Duffield *et al.*, 1984; González-Lara, 1994; García-Palomo *et al.*, 2004). These sequences are folded and form the Caimba and La Unión anticlines between the Buena Vista syncline (García-Palomo *et al.*, 2004) (Fig. 2). According to these authors, the area is cut by three fault systems: 1) a dextral strike-slip N-S set, 2) a sinistral strike-slip E-W set, and a normal N45°E set called Chapultenango Fault System. The E-W San Juan Fault system passes under El Chichón volcano and may be related to the extrusion of the Chapultenango basalt. The Chapultenango Fault system produced a half-graben geometry of blocks, on top of which El Chichón has been emplaced (Macías *et al.*, 1997a: García-Palomo *et al.*, 2004). The structural analysis of the sedimentary rocks indicates that during the Late Miocene, the El Chichón area has been subjected to a maximum principal stress (σ1) orientated N70°E, a minimum principal stress (σ3) orientated N20°W, and a vertical intermediate principal stress. This stress pattern has generated strike–slip motion and crustal earthquakes (<40 km) with sinistral strike-slip focal mechanisms orientated along the major faults (Guzmán-Speziale *et al.*, 1989) and suggests that the same tectonic regime has been occurring in southern Mexico from the Late Miocene to the Recent, controlling the emplacement and activity of El Chichón (García-Palomo *et al.*, 2004).

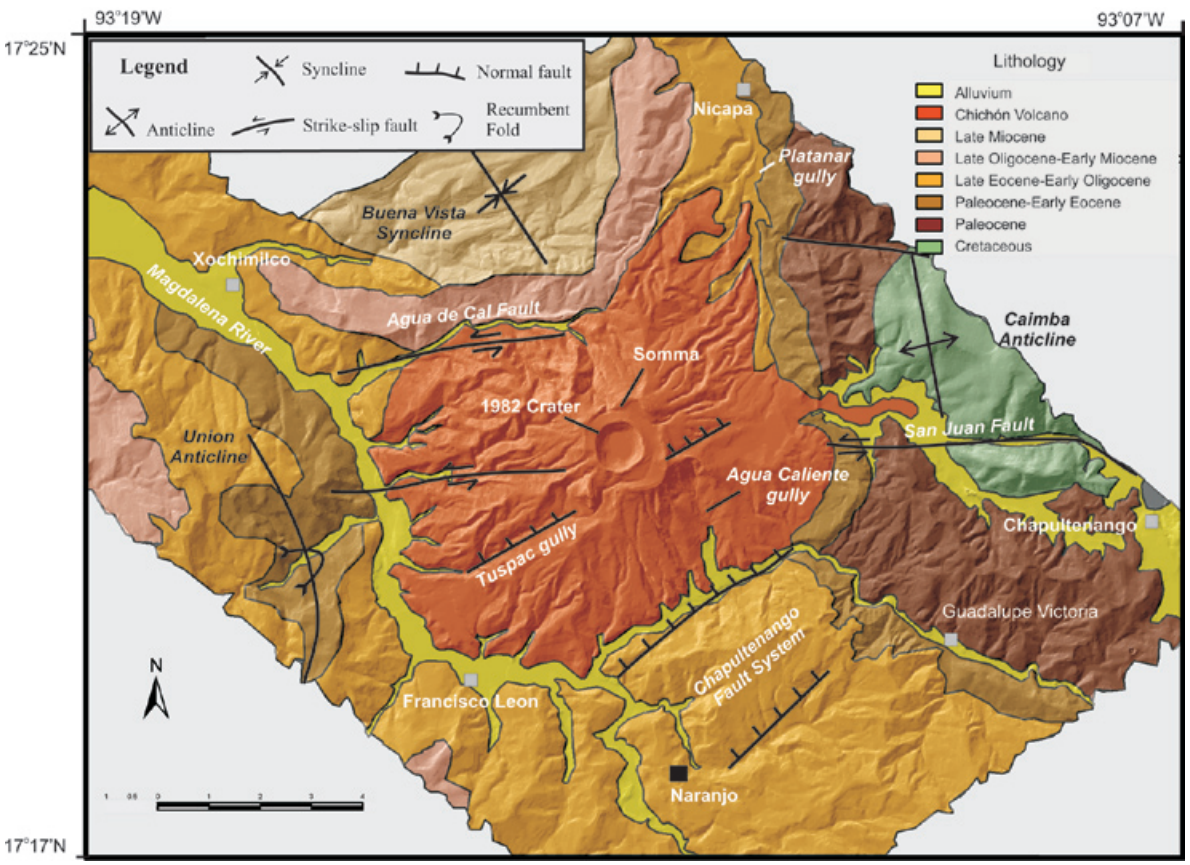

Fig. 2. Simplified geologic map of El Chichón Volcanic Complex and main structures on a shade relief map after García-Palomo *et al.* (2004) and Macías (2007).

Methodology

The geological map of El Chichón volcano presented in this paper is the result of a multidisciplinary approach to mapping in a highly vegetated, inaccessible region where the geomorphology has been changed rapidly following the 1982 eruption and subsequent erosion of the volcanic products. Initially, a photogeological interpretation of the area both before and after the 1982 eruption was carried out through the analysis of aerial photographs at a scale of 1:35,000 taken by DETENAL (Dirección General de Estudios del Territorio Nacional) in February 1978, and another set of photographs at a scale of 1:75,000 taken by DGG (Dirección General de Geografía) in 1984. In addition, two topographic maps of the area were used: the 1981 topographic map (E15C39, scale 1:50,000) published by INEGI (Instituto Nacional de Estadística Geografía e Informática) and a 1:50,000 topographic map produced by GYMSA using the 1984 aerial photography from DGG. The photogeological information obtained (volcanic structures, contacts, drainages, etc.) was merged with the topographic maps of the area to generate a relief model of the area using ARCGIS 9.3 and SURFER 8 commercial software. In addition we analyzed a Landsat TM image using bands 1, 2, 3, 4, 5 and 7, in order to identify morpholineal features and lithologic contacts between units. To calculate the areas occupied by the volcanic units described in this paper, we used the AUTOCAD 2005 and ARCGIS 9.3 programs. We determined the volumes of these units by combining thicknesses measured in the field with the areas using these programs.

We have conducted field mapping in the region from 1992 through 2007. Over this time we have constructed more than 500 stratigraphic sections, described over 200 structural sites, and collected samples for ^{14}C, K-Ar, and $^{40}Ar/^{39}Ar$ dating and other types of analysis (i.e., whole-rock chemistry of juvenile products). During these 17 years of work on El Chichón area, papers have been published on the structural geology of the volcano (García-Palomo *et al*., 2004), the volcanic stratigraphy (Macías *et al*., 1997b), petrological aspects (Espíndola *et al*., 2000; Macías *et al*., 2003; Jones *et al*., 2008; Andrews *et al*., 2008), and social effects of the eruption (Espíndola *et al*., 2002; Limón and Macías, this issue). A hazard map of the volcano (Macías *et al*., 2008) has also been published. Along with the study of the volcanic products, we have also mapped older sedimentary units shown in fig. 2 (García-Palomo *et al*., 2004).

Sample collection and $^{40}Ar/^{39}Ar$ analytical methods

Twelve samples from El Chichón volcano were acquired by the Geochronology Laboratory at the University of Alaska Fairbanks for the purposes of $^{40}Ar/^{39}Ar$ analysis (Fig. 3; Table 1). The majority were sent from the collections of the Universidad Nacional Autónoma de México, while CHI-SOMMA was collected during a reconnaissance campaign in 2005.

The samples were crushed, washed, sieved and hand-picked for small whole-rock chips suitable for dating. The monitor mineral TCR-2 with an age of 27.87 Ma (Lanphere and Dalrymple, 2000) was used to monitor neutron flux and calculate the irradiation parameter, J, for all samples. The samples and standards were wrapped in aluminum foil and loaded into aluminum cans of 2.5 cm diameter and 6 cm height. All samples were irradiated in position 5c of the uranium-enriched research reactor of McMaster University in Hamilton, Ontario, Canada for 0.5 (0.75 in the case of CHI-9521 and CHI-SOMMA) megawatt-hours.

Upon their return from the reactor, the whole rock chips and grains of the monitor mineral were loaded into 2 mm diameter holes in a copper tray that was then loaded in an ultra-high vacuum extraction line. The monitors were fused, and samples heated, using a 6-watt argon-ion laser following the technique described in York *et al*. (1981), Layer *et al*. (1987) and Layer (2000). Argon purification was achieved using a liquid nitrogen cold trap and a SAES Zr-Al getter at 400°C for 20 minutes. The samples were analyzed in a VG-3600 mass spectrometer controlled by either a LabView or Visual Basic operating program written in-house. The measured argon isotopes were corrected for system blank and mass discrimination, and for the irradiated samples, calcium, potassium and chlorine interference reactions, following procedures outlined in McDougall and Harrison (1999). System blanks generally were 2×10^{-16} mol ^{40}Ar and 2×10^{-18} mol ^{36}Ar, which are 5 to 50 times smaller than fraction volumes. Mass discrimination was monitored by running both calibrated air shots and a zero-age glass sample. These measurements were made on a weekly to monthly basis to check for changes in mass discrimination.

$^{40}Ar/^{39}Ar$ results

Fig. 3 shows the age, Ca/K, and Cl/K spectra as well as inverse isochron plots for the dated samples, and summary of the results is provided in Table 1. The raw data for the argon analyses are shown in Appendix 1. All ages are quoted to the 1-sigma level and calculated using the constants of Steiger and Jaeger (1977). The integrated age is the age given by the total gas measured and is equivalent to a potassium-argon (K-Ar) age. The age spectrum provides a plateau age if three or more consecutive gas fractions represent at least 50% of the total gas release and are within two standard deviations of each other (Mean Square Weighted Deviates less than

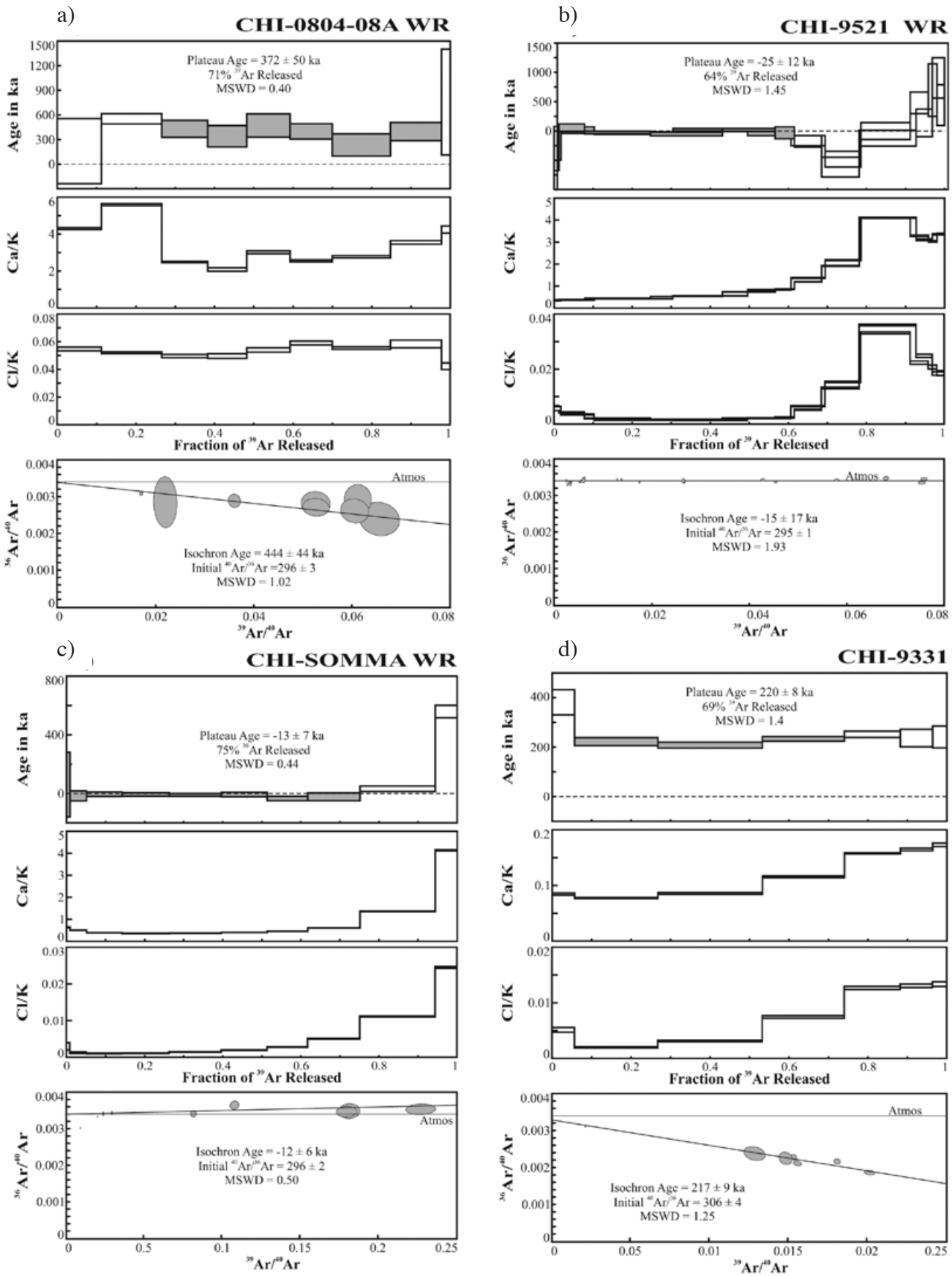
a)
CHI-0804-08A WR
Plateau Age = 372 ± 50 ka
71% 39Ar Released
MSWD = 0.40
Age in ka
Ca/K
Cl/K
Fraction of 39Ar Released
Atmos
Isochron Age = 444 ± 44 ka
Initial 40Ar/36Ar =296 ± 3
MSWD = 1.02
36Ar/40Ar
39Ar/40Ar
b)
CHI-9521 WR
Plateau Age = -25 ± 12 ka
64% 39Ar Released
MSWD = 1.45
Age in ka
Ca/K
Cl/K
Fraction of 39Ar Released
Atmos
Isochron Age = -15 ± 17 ka
Initial 40Ar/36Ar = 295 ± 1
MSWD = 1.93
36Ar/40Ar
39Ar/40Ar
c)
CHI-SOMMA WR
Plateau Age = -13 ± 7 ka
75% 39Ar Released
MSWD = 0.44
Age in ka
Ca/K
Cl/K
Fraction of 39Ar Released
Atmos
Isochron Age = -12 ± 6 ka
Initial 40Ar/36Ar = 296 ± 2
MSWD = 0.50
36Ar/40Ar
39Ar/40Ar
d)
CHI-9331
Plateau Age = 220 ± 8 ka
69% 39Ar Released
MSWD = 1.4
Age in ka
Ca/K
Cl/K
Fraction of 39Ar Released
Atmos
Isochron Age = 217 ± 9 ka
Initial 40Ar/36Ar = 306 ± 4
MSWD = 1.25
36Ar/40Ar
39Ar/40Ar

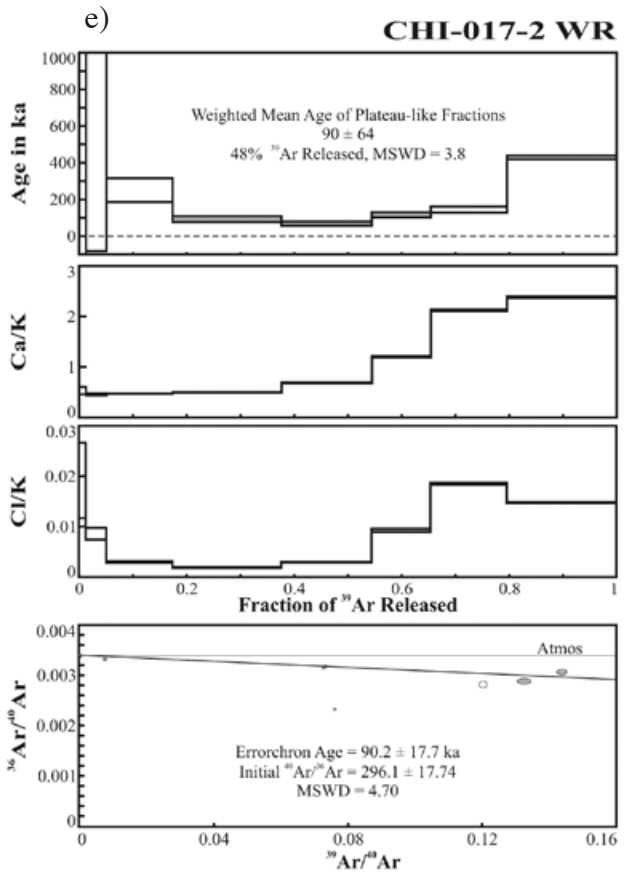
e)
CHI-017-2 WR
Age in ka
Weighted Mean Age of Plateau-like Fractions
90 ± 64
48% 39Ar Released, MSWD = 3.8
Ca/K
Cl/K
Fraction of 39Ar Released
36Ar/40Ar
Atmos
Errorchron Age = 90.2 ± 17.7 ka
Initial 40Ar/36Ar = 296.1 ± 17.74
MSWD = 4.70
39Ar/40Ar

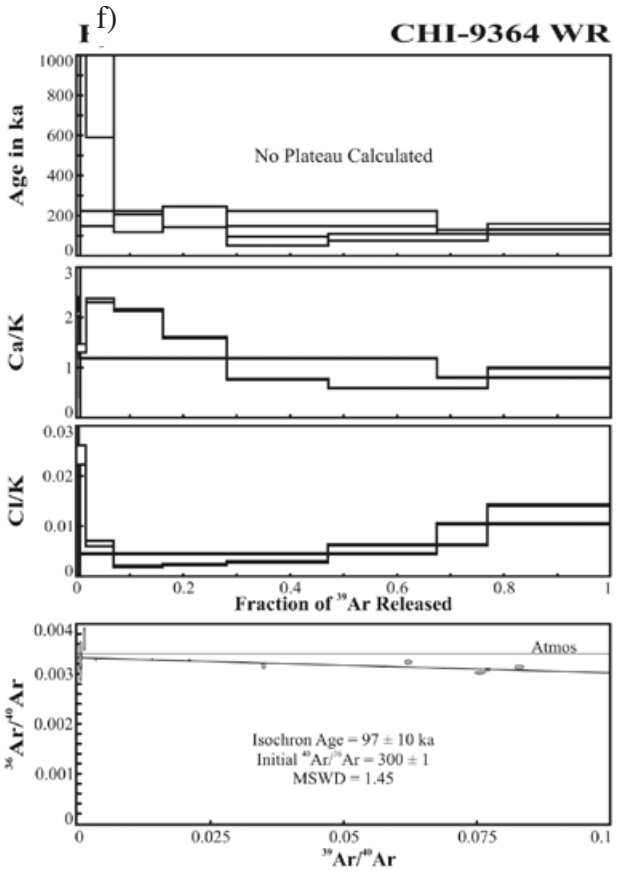
f)
CHI-9364 WR
Age in ka
No Plateau Calculated
Ca/K
Cl/K
Fraction of 39Ar Released
36Ar/40Ar
Atmos
Isochron Age = 97 ± 10 ka
Initial 40Ar/36Ar = 300 ± 1
MSWD = 1.45
39Ar/40Ar

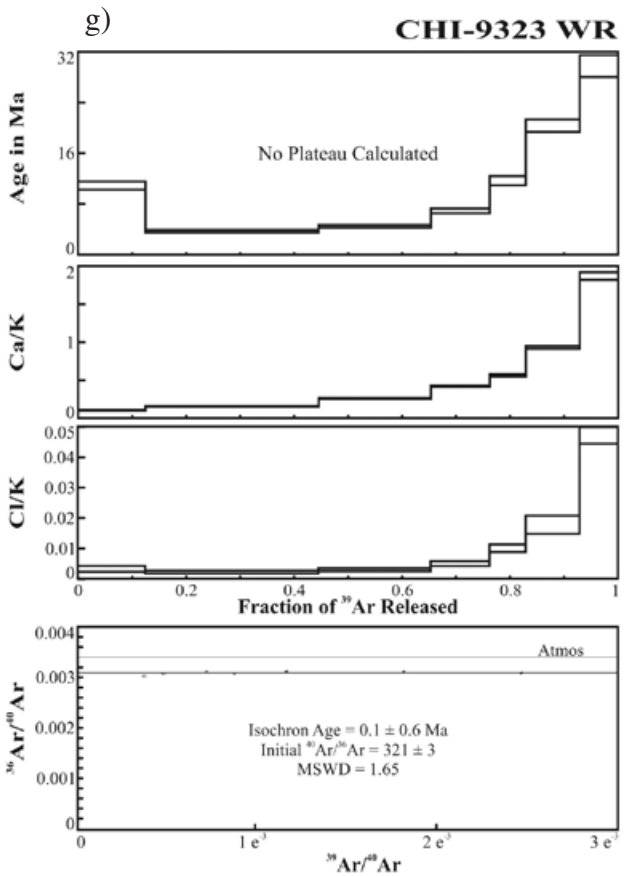
g)
CHI-9323 WR
Age in Ma
No Plateau Calculated
Ca/K
Cl/K
Fraction of 39Ar Released
36Ar/40Ar
Atmos
Isochron Age = 0.1 ± 0.6 Ma
Initial 40Ar/36Ar = 321 ± 3
MSWD = 1.65
39Ar/40Ar

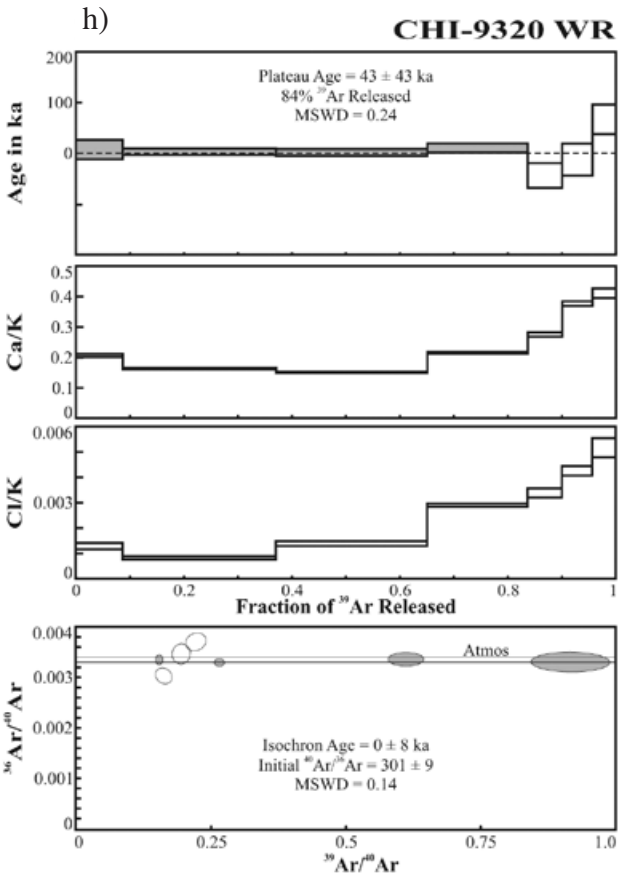
h)
CHI-9320 WR
Age in ka
Plateau Age = 43 ± 43 ka
84% 39Ar Released
MSWD = 0.24
Ca/K
Cl/K
Fraction of 39Ar Released
36Ar/40Ar
Atmos
Isochron Age = 0 ± 8 ka
Initial 40Ar/36Ar = 301 ± 9
MSWD = 0.14
39Ar/40Ar

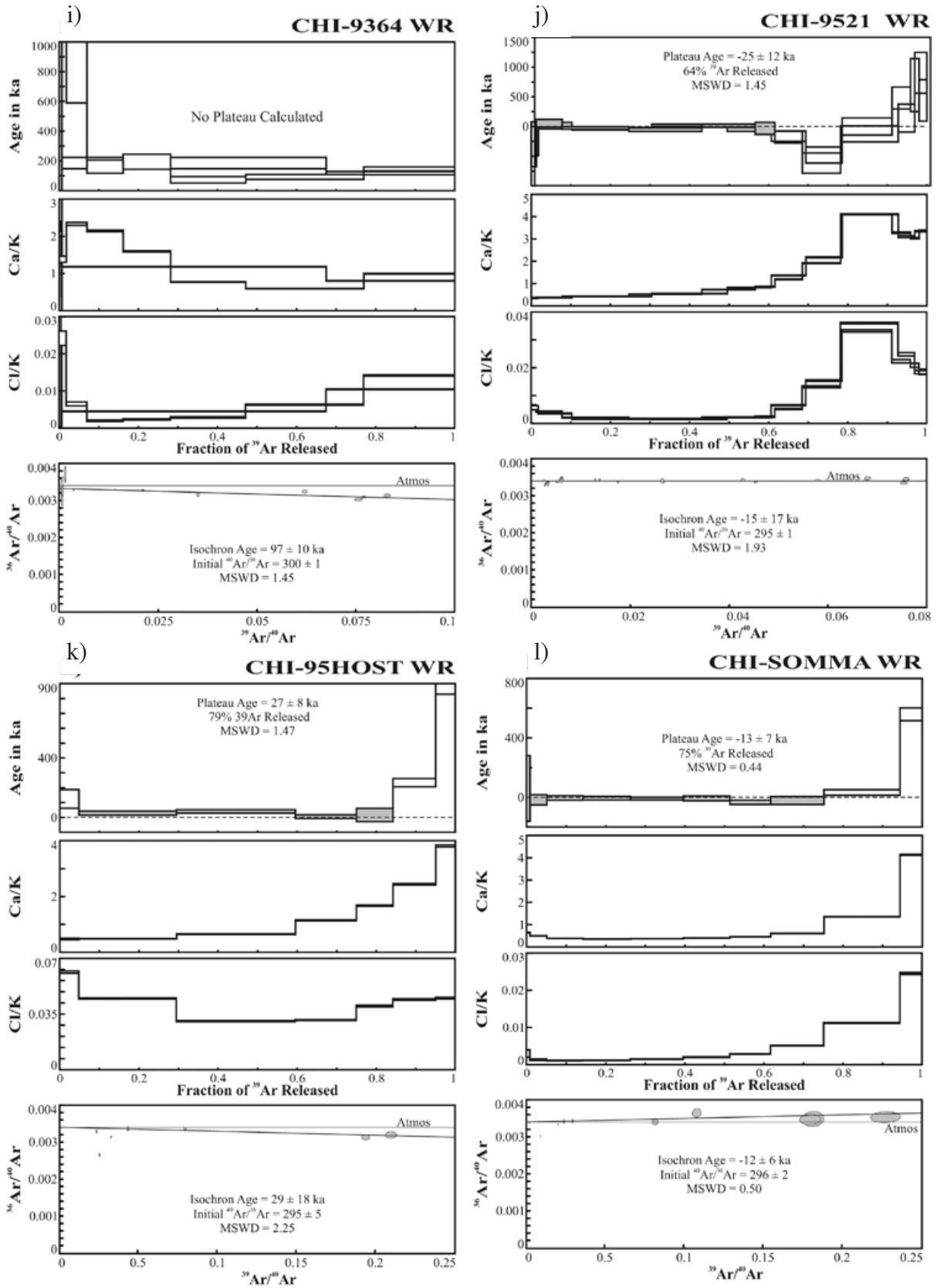

Fig. 3. (a-l) Age, Ca/K and Cl/K spectra, as well as inverse isochron diagrams, for twelve samples from EL Chichón Volcanic Complex. Spectra fractions and error ellipses are ± 1-sigma. Note that only the grey filled data point error ellipses used in the isochron regression, and only the grey filled steps were used in calculating the plateau and weighted mean ages.

~2.5). If the age spectrum did not provide a good plateau, the weighted mean age of any 'plateau-like' steps was calculated in lieu of a plateau age. The isochron age is proportional to the X-intercept of the best-fit regression of the data on an isotope correlation diagram; the Y-intercept is the inverse of the initial $^{40}Ar/^{36}Ar$ ratio.

Jones *et al*. (2008) reported the presence of excess argon in phenocryst phases in younger El Chichón eruptive products. Many of the samples show high Ca/K steps (Fig. 3), perhaps due to degassing of high Ca plagioclase microphenocrysts. Because of the possibility of excess argon in these older units, and because excess argon (initial $^{40}Ar/^{36}Ar$ ratios significantly greater than 295.5) is seen in some of the samples (Table 1), isochron ages were chosen as the preferred ages when possible (highlighted in bold in Table 1), although for most samples plateau ages are within 2-sigma of the isochron ages. These interpreted ages are shown in Table 1 and Fig. 3.

Six samples (CHI-95HOST, CHI-0804-08B, CHI-017-2, CHI-9364, CHI-9331, and CHI-0804-08A; Table 1) yielded statistically significant non-zero ages, while the other six (samples CHI-0804-01, CHI-0804-04,

Table 1

Summary of whole rock $^{40}Ar/^{39}Ar$ analyses. Bold print denotes preferred age (isochron vs plateau) for each sample. All ages are quoted to the ± 1-sigma level and calculated using the constants of Steiger and Jaeger (1977). *Analyses required multiple runs to produce statistically significant isochrons and/or plateaus.

Sample/ Location	Volcanic Unit	Integrated Age	Plateau (P) or Weighted –Mean (WM) Age	Plateau or Weighted – Mean Age Information	Isochron (I) or Errorchron (E) Age	Isochron or Errorchron Age Information
CHI-9323 17°21'09" N 93°12'36" W	Guayabal Tuff Cone	9.2 ± 0.2 Ma	-	-	**0.1 ± 0.6 Ma (I)**	**$^{40}Ar/^{36}Ar_i$ = 321 ± 3 5 of 7 fractions MSWD = 1.65**
CHI-9521* 17°21'40" N 93°12´40" W	Somma	-70 ± 32 ka (Run #1) -24 ± 29 ka (Run #2)	-25 ± 12 ka (P)	64% ^{39}Ar Released 10 of 22 fractions MSWD = 1.45	**-15 ± 17 ka (I)**	**$^{40}Ar/^{36}Ar_i$ = 295 ± 1 17 of 22 fractions MSWD = 1.93**
CHI-SOMMA	Somma	28 ± 7 ka	-13 ± 7 ka (P)	75% ^{39}Ar Released 8 of 10 fractions MSWD = 0.44	**-12 ± 6 ka (I)**	**$^{40}Ar/^{36}Ar_i$ = 296± 2 8 of 10 fractions MSWD = 0.50**
CHI-0804-04 17°21´26" N 93°13´26" W	1982 Crater	43 ± 12 ka	**-4 ± 9 ka (P)**	**88% ^{39}Ar Released 7 of 9 fractions MSWD = 1.48**	-	-
CHI-9320 17°21'28" N 93°13'03" W	Guayabal Tuff Cone	3 ± 5 ka	43 ± 43 ka (P)	84% ^{39}Ar Released 4 of 7 fractions MSWD = 0.24	**0 ± 8 ka (I)**	**$^{40}Ar/^{36}Ar_i$ = 301 ± 9 4 of 7 fractions MSWD = 0.14**
CHI-0804-01 17°21´40" N 93°13´49" W	1982 Crater	66 ± 8 ka	7 ± 33 ka (WM)	72% ^{39}Ar Released 3 of 9 fractions MSWD = 3.3	**8 ±11 ka (E)**	**$^{40}Ar/^{36}Ar_i$ = 294 ± 4 5 of 9 fractions MSWD = 4.46**
CHI-95HOST 17°21'50" N 93°12´37" W	Lithic in 1982 deposits	97 ± 8 ka	40 ± 12 ka (P)	79% ^{39}Ar Released 4 of 7 fractions MSWD = 1.47	**29 ± 18 ka (I)**	**$^{40}Ar/^{36}Ar_i$ = 295 ± 5 5 of 7 fractions MSWD = 2.25**
CHI-0804-08B 17°21´26" N 93°13´26" W	1982 Crater	154 ± 11 ka	67 ± 14 ka (P)	52% ^{39}Ar Released 4 of 7 fractions MSWD = 0.48	**44 ± 9 ka (I)**	**$^{40}Ar/^{36}Ari$ =303 ± 2 5 of 7 fractions MSWD = 0.69**
CHI-017-2 17°22'07" N 93°14'15" W	NW Dome	72 ± 72 ka	90 ± 64 ka (WM)	48% ^{39}Ar Released 3 of 8 fractions MSWD = 3.8	**90 ± 18 ka (E)**	**$^{40}Ar/^{36}Ar_i$ = 296 ± 18 6 of 8 fractions MSWD = 4.70**
CHI-9364* 17°22'52" N 93°14'55" W	NW Dome	178 ± 27 ka (Run #1) 207 ± 21 ka (Run #2)	-	-	**97 ± 10 ka (I)**	**$^{40}Ar/^{36}Ari$ = 300 ± 1 14 of 14 fractions MSWD = 1.45**
CHI-9331 17°21'16" N 93°14'06" W	SW Dome	236 ± 7 ka	220 ± 8 ka (P)	69% ^{39}Ar Released 3 of 7 fractions MSWD = 1.40	**217 ± 9 ka (I)**	**$^{40}Ar/^{36}Ar_i$ = 306 ± 4 7 of 7 fractions MSWD = 1.25**
CHI-0804-08A 17°21´26" N 93°13´26" W	Pre Somma	384 ± 60 ka	372 ± 5 ka (P)	**71% ^{39}Ar Released 6 of 9 fractions MSWD = 0.40**	444 ± 44 ka (I)	$^{40}Ar/^{36}Ari$ =296 ± 3 9 of 9 fractions MSWD = 1.02

CHI-9320, CHI09323, CHI-9521 and CHI-SOMMA) are irresolvable from zero age due to small amounts of radiogenic argon. While it is difficult to assign ages to these very young samples, based on the error on the most precise isochrons, we estimate that the samples are probably less than 10,000 years old.

Units of El Chichón Volcanic Complex

Based on the analysis of aerial photographs and satellite image supported by field mapping and description of the volcanic units we were able to define six volcanic units of the El Chichón Volcanic Complex. These units are informally called Pre-Somma, Somma Edifice, the SW Dome, the NW Dome, the Guayabal Tuff Cone, and the Holocene tuff cone that includes the 1982 crater. Each volcanic unit has distinctive morphology and drainage pattern allowing us to uniquely identify and map the units. In order to define the chronological position of these units during the evolution of El Chichón Volcanic Complex we collected samples for chemical analysis and $^{40}Ar/^{39}Ar$ dating. The units are described below as shown in fig. 4.

Pre-Somma

As revealed by aerial photographs and landsat image analysis there are two areas of older undifferentiated rocks that outcrop outside the Somma Edifice (Fig. 4). These two areas have developed deep dendritic drainages and can be isolated from the other units. Sample CHI-0804-08A, an accidental lithic collected from the 1982 pyroclastic products exposed at the top of the 1982 crater produced a plateau age of 372 ± 5 ka (Fig. 3a). The isochron calculated for the sample indicates an initial $^{40}Ar/^{36}Ar$ indistinguishable from atmospheric thus the age is interpreted to represent xenolithic contamination of the most recent eruption from the volcanic substrate. The most likely source for this lithic fragment is from these undifferentiated units (not mapped yet) that represent an older period of volcanic activity at El Chichón at least 370 ka. These units represent so far the oldest exposed structures of El Chichón Volcanic Complex.

Somma Edifice

The Somma rises from surrounding elevations of 600 m in the east and 200 m in the west. The Somma crater is ~1.5 km wide and has inner steep slopes and external gentle slopes with a maximum elevation of 1150 m above sea level. This crater has three main notches that form the gorge heads of the El Platanar Valley to the east, the San Pablo-Cambac Valley to the north, and the Tuspac Valley to the southwest. The Somma crater rim consists of an amalgamation of steep dome extrusions of porphyritic andesites surrounded by an apron of block-and-ash flow deposits. The Somma edifice covers an area of ~40 km^2 and has an estimated volume of ~18 km^3.

Prior to the 1982 eruption, Damon and Montesinos (1978) reported a whole-rock K-Ar age of 209 ± 19 ka from a sample of "dacite" collected at the moat area at an elevation of 950 m above sea level. According to the authors' description this sample was taken at the moat area likely at the base of the eastern wall of the Somma crater. After the 1982 eruption, Duffield *et al*. (1984) dated another sample of the eastern wall rocks of the Somma crater at 276 ± 6 ka, significantly older than the age obtained by Damon and Montesinos (1978). This sample is a dome rock with a chemical composition of 57.8 wt. % SiO_2 (McGee *et al*., 1987) and falls in the alkaline series of figure 6 within the trend of most rocks of El Chichón.

As mentioned above, the flanks of the Somma crater consist of highly indurated, gray, massive block-and-ash flow deposits with lapilli-and-block-clasts (unit E of Tilling *et al*., 1984) interbedded with lahar deposits. These deposits are widely distributed around the volcano and probably arose from the events that built up the Somma crater and contribute significantly to the overall morphology of the volcano. In addition, a gray porphyritic lava flow rich in plagioclase and hornblende phenocrysts was described as unit M by Espíndola *et al*. (2000). Whole-rock chemical analyses indicate that this lava flow is andesitic in composition (CHI-9521; 58.9 % SiO_2; Table 2). This lava flow (Fig. 3b) and another sample (CHI-SOMMA; Fig. 3c) collected at a dome near the east-southeastern rim of the Somma crater, yielded Holocene ages with large standard deviations (Table 1) implying that the Somma Edifice could have been reactivated during the Holocene.

SW Dome

This structure was first described as a lateral flank dome (Canul and Rocha, 1981; Duffield *et al*., 1984), and as the SW Dome by Macías *et al*. (1997a). This dome has a maximum elevation of 990 m with 300-m high subvertical walls poorly incised by drainage (Fig. 4). Extrusion of the SW Dome disrupted the southwestern rim of the Somma Crater. The SW Dome covers an area of 0.32 km^2 and has an approximated volume of 0.1 km^3. The dome rock is a massive partly altered porphyritic andesite (58.2 wt. % SiO_2) (Table 2). Sample CHI-9331 is an andesite composed of plagioclase, hornblende and pyroxene in a glassy matrix, collected from the summit of the dome and gave an isochron age of 217 ± 9 ka displaying slight amounts of excess initial $^{40}Ar/^{36}Ar$ (Fig. 3d).

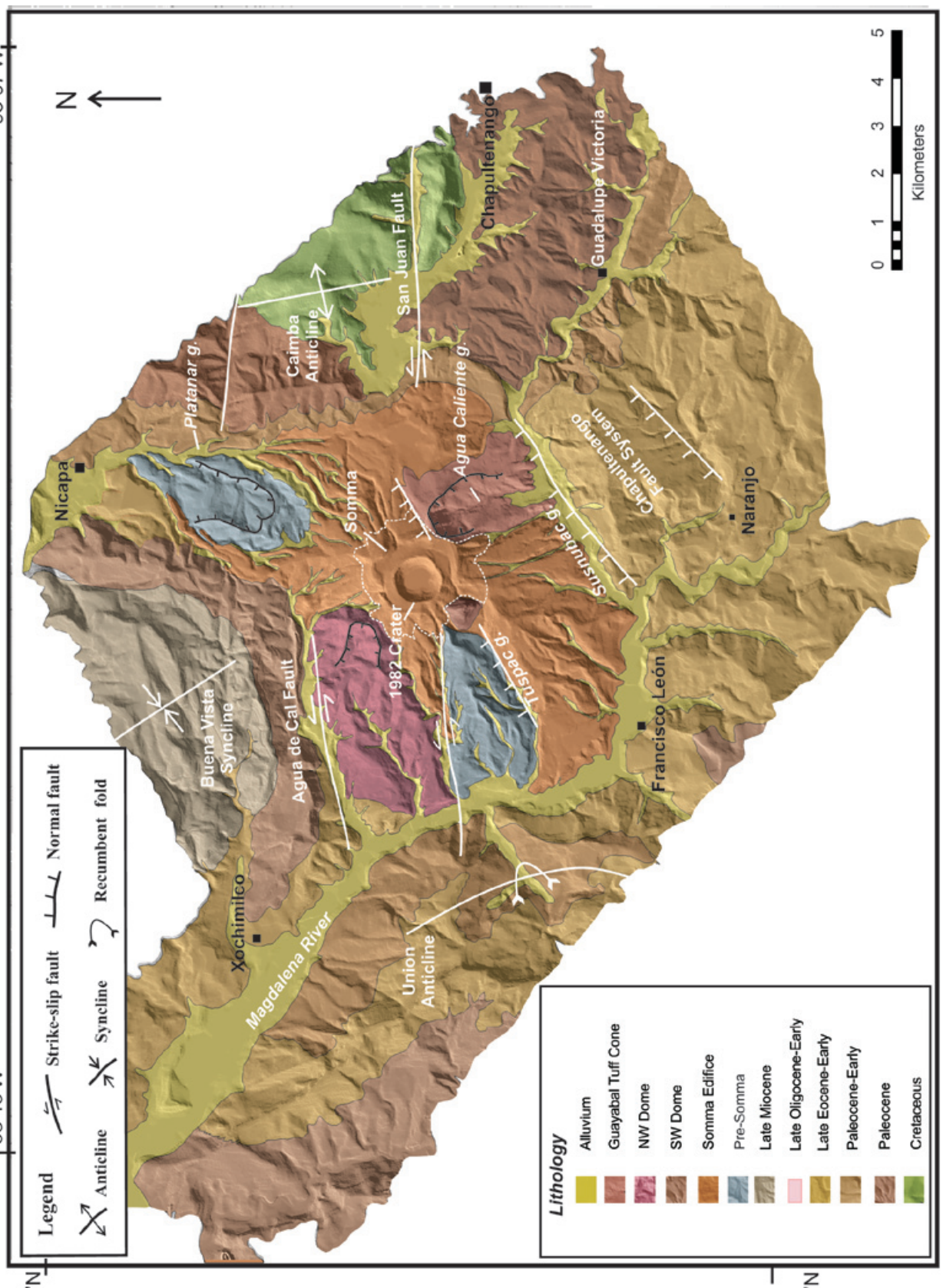

Fig. 4. Geological map of major volcanic units of El Chichón Volcanic Complex over a shade relief map showing main collapse scars and simplified stratigraphic column.

Table 2

Whole-rock chemical analysis of volcanic units of El Chichón Volcanic Complex performed at *ACTLABS, LTD, Canada and LUGIS of the Instituto de Geología, UNAM (Lozano *et al*., 1995). For sample location see Table 1.

Sample Units	**CHI0804-04 1982 crater**	**CHI-08-08B Pre-1982 crater**	**CHI0172 NW Dome**	**CHI0173 NW Dome**	**CHI0101 Post-Somma**	**CH197SW SW Dome**	**CHI0804-03 1982 crater**	**CH0804-08A Pre-Somma**
wt. %								
SiO_2	57.45	57.23	55.34	56.28	46.71	58.19	58.08	56.37
Al_2O_3	18.37	18.66	19.62	18.3	13.82	17.39	18.61	18.1
Fe_2O_3	6.35	6.58	7.25	6.77	12.07	5.98	6.34	6.33
MnO	0.18	0.17	0.18	0.18	0.402	0.14	0.12	0.17
MgO	2.11	2.18	2.15	2.44	7.48	1.95	2.05	2.05
CaO	7.63	7.33	8.04	8.01	12.06	6.76	6.22	7.34
Na_2O	4.01	3.95	3.7	4.06	2.9	3.78	4.23	3.96
K_2O	2.67	2.63	2.02	2.43	1.31	2.72	3.02	2.73
TiO_2	0.67	0.68	0.71	0.69	1.14	0.63	0.66	0.66
P_2O_5	0.31	0.32	0.41	0.29	nd	0.26	0.19	0.32
LOI	0.14	0.13	0.64	0.34	0.67	0.27	0.33	1.94
Total	99.89	99.86	100.06	99.79	98.87	98.06	99.85	99.97
ppm								
Sr	1066	920	1158	957	695	923	1072	1048
Ba	810	748	636	708	417	760	792	772
Y	31	33	22	18	23	19	25	33
Zr	185	170	180	117	98	128	186	187
Co	39	51	23	13.8	40.9	11.3	37	42
Cr	7	11	5	7.6	374	11.8	9	19
Cs	n.d.	n.d.	n.d.	1.9	1.5	2.1	n.d.	n.d.
Hf	n.d.	n.d.	n.d.	2.9	4.5	3.6	n.d.	n.d.
Rb	90	87	60	74	35	74	77	95
Sb	n.d.	n.d.	n.d.	0.3	0.2	0.3	n.d.	n.d.
Sc	n.d.	n.d.	n.d.	11.6	21.7	10.1	n.d.	n.d.
Ta	n.d.	n.d.	n.d.	2.9	0.3	0.7	n.d.	n.d.
Th	7	6	4	6.8	2	7.6	6	8
U	n.d.	n.d.	n.d.	2.5	0.8	2.3	n.d.	n.d.
La	n.d.	n.d.	n.d.	27.8	24.5	30.7	n.d.	n.d.
Ce	n.d.	n.d.	n.d.	52	55	59	n.d.	n.d.
Nd	n.d.	n.d.	n.d.	23	28	26	n.d.	n.d.
Sm	n.d.	n.d.	n.d.	4.42	5.66	4.66	n.d.	n.d.
Eu	n.d.	n.d.	n.d.	1.4	1.62	1.29	n.d.	n.d.
Tb	n.d.	n.d.	n.d.	0.5	0.7	0.6	n.d.	n.d.
Yb	n.d.	n.d.	n.d.	1.76	2.63	1.9	n.d.	n.d.
Lu	n.d.	n.d.	n.d.	0.25	0.38	0.3	n.d.	n.d.
Cu	24	28	24	18	42	27	119	44
Pb	6	6	7	10	3	11	9	8
Zn	67	74	68	76	118	77	70	80
Ni	11	14	6	1	74	5	7	12
V	142	175	156	173	246	157	171	159
Nb	18	21	25	n.d.	n.d.	n.d.	19	20

*Major and trace elements analyzed by Inductively Coupled Plasma Mass Spectrometry (ICP-MS) and Instrumental Neutron Activation Analysis (INAA) (<0.01% major elements; Ba, 50 ppm; Cr, Pb, Nb, V, and Rb, 2 ppm; Ni, Sc, Sr, Y, and Zr, 1 ppm; Cu, Zn and Ta, 0.5 ppm; Hf and Th, 0.2 ppm; U, 0.1 ppm; La, Ce, Nd, Sm, Tb and Yb, 0.1 ppm; Eu, 0.05 ppm, detection limits) at Activation Laboratories, Ancaster, Canada.

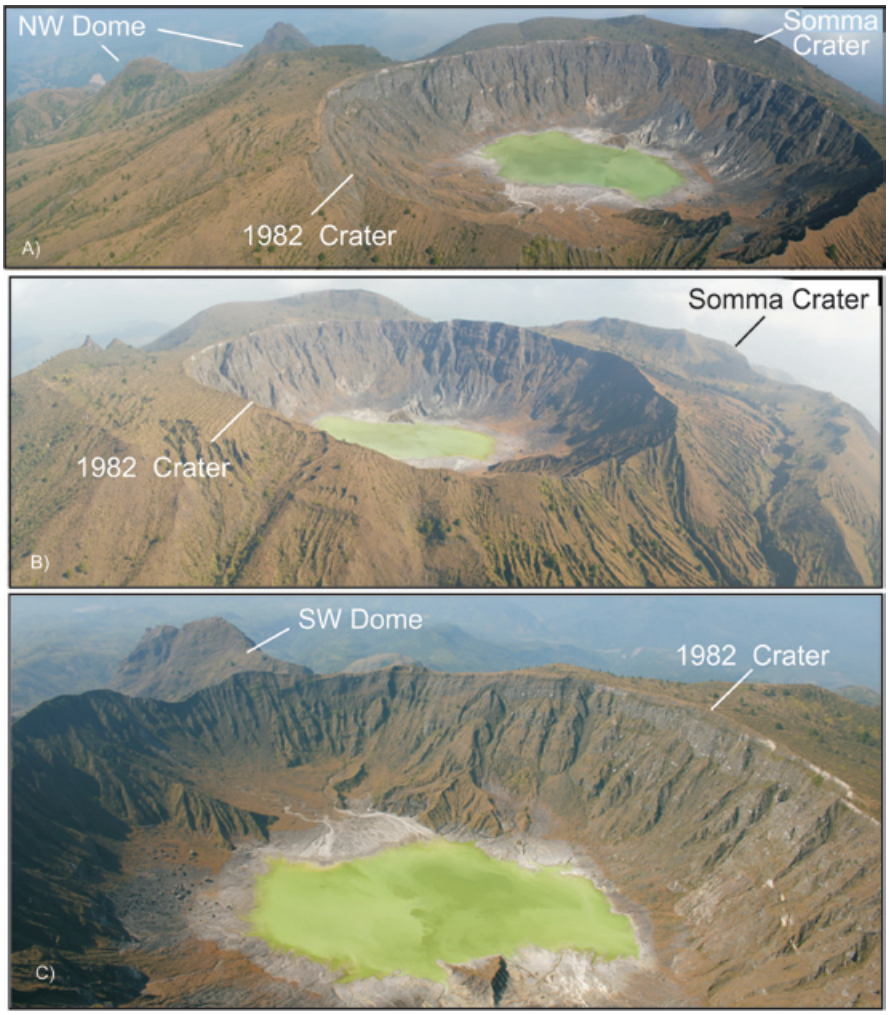

Fig. 5. Aerial views to the NW (a) and N (b) of El Chichón Volcanic Complex showing the Somma crater, NW Dome, and (c) the 1982 crater. Photographs taken in January 2008 by J.L. Macías.

NW Dome

This unit was described by Macías (1994) and Macías *et al*. (1997a) as the NW Dome. It consists of a dome structure with a maximum elevation of 1048 m. above sea level. The photogeological map shows that the NW Dome is highly eroded with a deep incised drainage and a ~700 m wide collapse structure opened to the NW (Figs. 3 and 4). The NW Dome covers an area of ~5 km^2 with an estimated volume of ~3 km^3 and is composed of gray to green partially altered andesitic lavas. We analyzed two different rocks from this structure. Sample CHI-017-2 a porphyritic andesite (56.3 wt. % SiO_2; Fig. 3e, Table 2) collected at the base of the dome near the NW rim of the Somma crater, and sample CHI-9364 was collected along the Cambac Gully. These rocks produced identical (within error) isochron ages of 90 ± 18 ka, and 97 ± 10 ka, respectively (Fig. 3f).

Guayabal Tuff Cone

This unit is represented by the remains of the Guayabal Tuff Cone. This cone has a horseshoe shaped crater open to the south into the Agua Caliente gully (Fig. 4). The tuff cone rests on top of the extrusive rocks of the Somma Edifice. The Guayabal cone has a maximum elevation of 950 m and it is ~700 m wide. The northeastern wall of the Guayabal Tuff Cone exposes at least three thick undifferentiated pyroclastic units with a pyroclastic surge on top. The latter contains white boulders of Cretaceous limestones from the volcano basement. The base of the Guayabal cone is exposed at the Agua Caliente gully upon andesite of the Somma crater. Here the andesites host abundant limestone xenoliths and trachybasaltic enclaves (CHI9505; 59.1 wt. % SiO_2; Table 2).

Two samples collected at the crater summit and at northwestern flanks of the Guayabal Tuff Cone were dated. Sample CHI-9320 (summit) is a porphyritic andesite with mm-size plagioclase crystals and sample CHI-9323 (flank) a porphyritic andesite with plagioclase and hornblende. The flank sample (CHI-9323) collected from the dome rock forming the substrate of the Guayabal Tuff Cone yielded an imprecise age (due to a very high atmospheric argon signal) of 100 ± 600 ka, which does not provide any useful age constraint (Fig. 3g; Table 1). However the summit sample (CHI-9320), taken from a pyroclastic surge deposit below the 1982 products gave an age of 0 ± 8 ka (Fig. 3h), indistinguishable from zero and implies that the deposit is probably less than 10 thousand years old and suggests that the Guayabal Tuff Cone could have been active during the Holocene.

Holocene tuff cone

The youngest unit of El Chichón Volcanic Complex is a tuff cone located at the center of the Somma crater and is Holocene in age. This area has been the focus of activity of El Chichón volcano during the Holocene with the occurrence of at least 12 explosive events (Espíndola *et al.*, 2000) and is now the site of the 1982 crater (Fig. 4). These explosive events have erupted magmas with a chemical composition varying from 55.18 to 58.8 wt. % SiO_2 falling within the trachyandesitic field of fig. 6 (Table 2).

Prior to the 1982 eruption this tuff cone was filled by a 1230 m high dome with two summit bulges. During dome growth, a 1.5 km long lava flow overflowed the SW flank of the Somma crater. The 1982 eruption destroyed the central dome and produced a 1 km wide crater with a maximum elevation of 1,000 m. This crater has vertical inner walls up to 140 m deep, with its floor sitting at an elevation of 860 m hosts a lake, fumaroles, mud and boiling water ponds (Taran *et al.*, 1998; Tassi *et al.*, 2003; Rouwet *et al.*, 2004). The products of the 1982 crater extend all around El Chichón Volcanic Complex pyroclastic flows and surges destroyed ca. 100 km^2 of jungle. These deposits contain a large variety of juvenile and accidental blocks from the volcanic conduit and crater walls.

For this study we collected five samples associated to the 1982 crater rocks or pyroclastic products. Samples CHI-0804-01, CHI-0804-04, CHI-0804-08A and CHI0804-08B were all collected from the walls of the 1982 eruption crater. Samples CHI-0804-01, and CHI-0804-04, are indistinguishable from zero age and probably less than 10,000 years old (Fig. 3i and j; Table 1) suggesting that renewed explosive activity has taken place in this crater at least during the Holocene. Samples CHI-0804-08A and CHI-0804-08B are accidental lithics collected from the 1982 pyroclastic products exposed at the top of the 1982 crater. Sample CHI-0804-08B has an isochron age of 44 ± 9 ka (Fig. 3k), while sample CHI-0804-08A (discussed above, Fig. 3a) produced a plateau

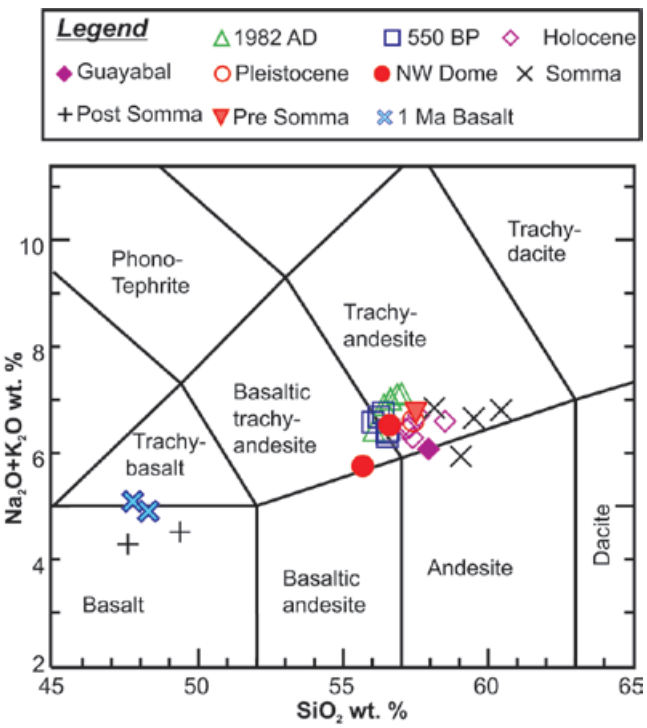

Fig. 6. TAS diagram of El Chichón rock samples. All data were recalculated on anhydrous basis (see Table 2 for source data).

age of 372 ± 5 ka. Another accidental lithic collected from the 1982 pyroclastic flow deposits at the Platanar gully (CHI-95HOST) has an isochron age of 29 ± 17 ka (Fig. 3l; Table 1).

Discussion and conclusions

Inception of volcanism in the area began 1.1 Ma with the extrusion of the Chapultenango basalt located at ~10 km east of El Chichón Volcanic Complex (García-Palomo *et al*., 2004). Although, this basalt is not directly linked to the activity of El Chichón, it lies at the eastern tip of the E-W strike slip San Juan Fault whose trace transects El Chichón Complex. Following a significant hiatus, volcanism shifted ~10 km to the west around the present location of El Chichón. The oldest age from our suite of samples is 372 ± 5 ka, for an accidental lithic that may represent the onset of edifice building related to the Pre-Somma undifferentiated volcanics. Further field mapping, geochemical and geochronological analyses are needed to better describe this early history.

As the edifice developed, the locus of magmatism focused at the Somma edifice and occurred between 209-276 ka (Damon and Montesinos, 1978; Duffield *et al*., 1984) through the emplacement of a dome complex. These ages seem to indicate that the main volcanic edifice is an amalgamation of volcanic domes extruded over the course of roughly 77 thousand years (and maybe as long as 150 thousand years). The episode of dome extrusion and evolution was accompanied by the generation of block-and-ash flows that reach up to 3 km from the vent to form an apron around the domes. These deposits were immediately or subsequently remobilized as lahars emplacing deposits interbedded with the block-and-ash flow deposits. The activity of the Somma dome complex continued during late Pleistocene with a major eruption that destroyed the central part of the complex forming a 1.5 km wide crater. Unfortunately, with the available information we are unable to ascertain the type and magnitude of this eruption. Finally, the last activity of the Somma crater occurred during the Holocene with the emission of a lava flow on the northeastern flank of the crater.

A new episode of dome extrusion occurred at the SW edge of the Somma that disrupted parts of the crater rim indicating that extrusion might have occurred some time after or contemporaneously with the formation of the Somma crater. Alternatively, Duffield *et al*. (1984) considered that this "flank dome" was associated with a 1.2 km wide crater, although the timing of formation of this crater was not constrained.

Between 216 and 95 ka, the volcanic complex entered into an apparent quiescent stage because no products of this age have been so far dated. Around 95 ka magmatism migrated 2.5 km to the northwest outside of the Somma crater with the extrusion of domes. The NW dome has been affected by a large collapse that left a horseshoe shaped crater open to the NW.

Between 95 ka and the Holocene appears to be another period of quiescence. The only evidence of activity during this time are ages of 44 ± 10 ka, and 29 ± 18 ka from accidental lithics from the 1982 eruption that do not seem to be associated with any exposed structures. It is also possible that these ages reflect partial resetting of older material due to incorporation of the lithics in the 1982 magma.

The next locus of activity migrated 3 km to the southeast at the SE edge of the Somma crater rim. This event marks an important shift in the activity of El Chichón volcanic complex with the establishment of explosive hydromagmatic eruptions that formed the Guayabal Tuff Cone. This cone is formed by at least three undifferentiated pyroclastic deposits, the youngest of which is Holocene and contains cm-size limestone xenoliths carried to surface by the hydromagmatic explosions. This deposit directly underlies the products of the 1982 eruption.

During the Holocene explosive activity returned to the Somma crater. This activity formed a ~1 km wide tuff crater (reactivated during the 1982 eruption) that has been the locus of volcanic activity during the past 8,000 years (Espíndola *et al*., 2000). This crater has produced 12 eruptions during this time span including the 1982 eruption. These eruptions have produced about 4 km^3 of trachyandesitic magma with an estimated average eruptive rate of 0.5 km^3/ka.

To better understand the evolution of El Chichón further field reconnaissance and geochronological data are needed in some areas around the complex that might preserve signs of older or intermediate activity.

Acknowledgments

This project was supported by grants from Consejo Nacional de Ciencia y Tecnología (27993-7 to J. L. M.), National Science Foundation (EAR-0408800 to P.W.L.). We appreciate the technical support provided by Celia López Miguel (UNAM) and Jeff Drake (UAF). We appreciate the thoughtful reviews made by Wendell Duffield and Peter Schaaf to this manuscript.

Bibliography

Andrews, B. J., J. E. Gardner and T. B. Housh, 2008. Repeated recharge, assimilation, and hybridization in magmas erupted from El Chichón as recorded by

plagioclase and amphibole phenocrysts. *J Volcanol. Geotherm. Res., 175*, 415-426.

Canul, R. F. and V. L. Rocha, 1981. Informe geológico de la zona geotérmica de "El Chichonal," Chiapas: Comisión Federal de Electricidad, Informe (Unpublished internal report).

Canul, R. F., A. M., Razo and V. L. Rocha, 1983. Geología e historia vulcanológica del Volcán Chichonal, Estado de Chiapas. El Volcán Chichonal. *Revista del Instituto de Geología, UNAM*: 3-22.

Carey, S. N. and H. Sigurdsson, 1986. The 1982 eruptions of El Chichón volcano, Mexico: 2. Observations and numerical modeling of tephra fall distribution. *Bull. Volcanol., 48*, 127-141.

Carroll, M. R. and M. T. J. Rutherford, 1987. The stability of igneous anhydrite. Experimental results and implications for sulfur behavior in the 1982 El Chichón trachyandesite and other evolved magmas. *J. Petrol., 28*, 781-801.

Casadevall, T. J., S. De La Cruz-Reyna, W. I. Rose, S. Bagley, D. L. Finnegan and W. H. Zoller, 1984. Crater lake and post-eruptions hydrothermal activity, El Chichón Volcano, Mexico. *J. Volcanol. Geotherm. Res., 23*, 169-191.

Damon, P. and E. Montesinos, 1978. Late Cenozoic volcanism and metallogenesis over an active Benioff Zone in Chiapas, Mexico. *Arizona Geological Society Digest, 11*, 155-168.

Devine, J. D., H. Sigurdsson, A. N. Daves and S. Self, 1984. Estimates of sulfur and chlorine yield to atmosphere from volcanic eruptions and potential climatic effects. *J. Geophys. Res., 89*, 6309-6325.

Duffield, W. A., R. I. Tilling and R. Canul, 1984. Geology of Chichón Volcano, Chiapas, Mexico. *J. Volcanol. Geotherm. Res., 20*, 117-132.

Espíndola, J. M., J. L. Macías, R. I. Tilling and M. F. Sheridan, 2000. Volcanic history of El Chichón Volcano (Chiapas, Mexico) during the Holocene, and its impact on human activity. *Bull. Volcanol., 62*, 90-104.

Espíndola, J. M., J. L. Macías, L. Godínez and Z. Jiménez, 2002. La erupción de 1982 del Volcán Chichónal, Chiapas, México, in Desastres Naturales en América Latina: Mexico, edited by H. J. Lugo and M. Inbar, Fondo de Cultura Económica, México D. F., 37-65.

García-Palomo, A., J. L. Macías and J. M. Espíndola, 2004. Strike-slip faults and K-Alkaline volcanism at El Chichón volcano, southeastern Mexico. *J. Volcanol. Geotherm. Res., 136*, 247-268.

García-Palomo, A., J. L. Macías, J. L. Arce, J. C. Mora, S. Hughes, R. Saucedo, J. M. Espíndola, R. Escobar and P. W. Layer, 2006. Geological evolution of the Tacaná Volcanic Complex, Mexico-Guatemala. In Volcanic Hazards in Central America, edited by W. I. Rose, G. J. S. Bluth, M. J. Carr, J. Ewert, L. Patino, and J. Vallance. *Geol. Soc. Amer. Special Paper, 412*, p. 39-57.

González-Lara, J. C., 1994. Estudio Bioestratigrafico de una secuencia arcillo-arenosa del Neogeno. Basado en foraminíferos plantónicos y bentónicos del sur de Veracruz y Noroeste de Chiapas. M. Sc. Thesis, Instituto Politécnico Nacional, Escuela Superior de Ingeniería y Arquitectura, México, D.F, 110 pp.

Guzmán-Speziale, M., W. D. Pennington and T. Matumoto, 1989. The triple junction of the North America, Cocos, and Caribbean plates. *Seism. Tect., 8*, 981- 997.

Jiménez, Z., V. H. Espíndola and J. M. Espíndola, 1998. Evolution of the Seismic Activity from the 1982 Eruption of El Chichón Volcano, Chiapas, Mexico: *Bull. Volcanol., 61*, 411-422.

Jones, D. A., P. W. Layer and R. J. Newberry, 2008. A 3100-year history of Argon isotopic and compositional variation at El Chichón Volcano. J. Volcanol. *Geotherm. Res., 175*: 427-443.

Lanphere, M. A. and G. B. Dalrymple, 2000. First-principles calibration of ^{38}Ar tracers: Implications for the ages of ^{40}Ar/^{39}Ar fluence monitors. U.S. *Geological Survey Professional Paper 1621*, 10 p.

Layer, P. W. 2000. Argon-40/argon-39 age of the El'gygytgyn impact event, Chukotka, Russia. *Meteoritics and Planetary Sciences, 35*, 591-599.

Layer, P. W., C. M. Hall and D. York, 1987. The derivation of ^{40}Ar/^{39}Ar age spectra of single grains of hornblende and biotite by laser step-heating. *Geophys. Res. Lett., 14*, 757-760.

Limón-Hernández, C. and J. L. Macías, 2009. Volcanic hazards and risk perception at the "Zoque" community of Chapultenango: El Chichón Volcano, Chiapas, México. *Geofís. Int. 48-1*, 113-132.

Luhr, J. F., 1991. Volcanic shade causes cooling. *Nature, 354*, 104-105.

Luhr, J. F., I. S. E. Carmichael and J. C. Varekamp, 1984. The 1982 eruptions of El Chichón Volcano, Chiapas, Mexico: mineralogy and petrology of the anhydrite-bearing pumices. *J. Volcanol. Geotherm. Res., 23*, 69-108.

Luhr, J. F. and M. V. A. Logan, 2002. Sulfur isotope systematics of the 1982 El Chichón trachyandesite: an ion microprobe study. *Geochim. Cosmochim. Acta, 66*, 3303-3316.

Macías, J. L., 1994. Violent short-lived eruptions from small-size volcanoes: El Chichón, Mexico (1982) and Shtyubel', Russia (1907): [Ph. D. thesis]: Buffalo, State University of New York at Buffalo, 193 p.

Macías, J. L., 2007. Geology and eruptive history of some active volcanoes of México, in Geology of México: Celebrating the Centenary of the Geological Society of México. Edited by S. A., Alaniz-Álvarez and Á. F., Nieto-Samaniego, *Geol. Soc. Amer. Special Paper 422*, p. 183–232.

Macías, J. L., J. M. Espíndola, T. Taran and A. García-Palomo, 1997a. Explosive volcanic activity during the last 3,500 years at El Chichón Volcano, Mexico. IAVCEI, General Assembly, Puerto Vallarta, Mexico. Field Trip Guide, 53 p.

Macías, J. L., M. F. Sheridan and J. M. Espíndola, 1997b. Reappraisal of the 1982 Eruptions of El Chichón volcano, Chiapas, Mexico: New data from the Proximal Deposits. *Bull. Volcanol., 59*, 459-471.

Macías, J. L., J. L. Arce, J. C. Mora, J. M. Espíndola, R. Saucedo and P. Manetti, 2003. The ~550 bp Plinian eruption of el Chichón volcano, Chiapas, Mexico: Explosive volcanism linked to reheating of a magma chamber. *J. Geophys. Res., 108, B12*, 2569 pp.

Macías, J. L., L. Capra, J. L. Arce, J. M. Espíndola, A. García-Palomo and M. F. Sheridan, 2008. Hazards map of El Chichón Volcano, Chiapas, México: Constraints posed by eruptive history and computer simulations. *J. Volcanol. Geotherm. Res., 175*, 444-458.

McDougall, I. and T. M. Harrison, 1999. Geochronology and Thermochronology by the $^{40}Ar/^{39}Ar$ method, Second Edition. Oxford University Press, 269 pp.

McGee, J. J., R. I. Tilling and W. A. Duffield, 1987. Petrologic characteristics of the 1982 and pre-1982 eruptive products of El Chichón volcano, Chiapas, Mexico. *Geof. Int., 26*, 85-10.

Meneses-Rocha, J. J., 1991. Tectonic Development of the Ixtapa Graben, Chiapas, Mexico. Ph. D., University of Texas, Austin, 308 pp.

Müllerried, F. K. G., 1933. El Chichón, único volcán en actividad descubierto en el estado de Chiapas. *Memorias de la Sociedad Científica Antonio Alzate, 54*, 411-416.

Nixon, G. T., 1982. The relationship between Quaternary volcanism in central Mexico and the seismicity and structure of the subducted ocean lithosphere. *Geol. Soc. Amer. Bull., 93*, 514-523.

Pardo, M. and G. Suárez, 1995. Shape of the subducted Rivera and Cocos plates in southern Mexico: Seismic and tectonic implications. *J. Geophys. Res., 100, B7*, 12,357-12,373.

Rampino, M. R. and S. Self, 1984. Sulphur-rich volcanic eruptions and stratospheric aerosols. *Nature, 310*, 677-679.

Rebollar, C. J., V. H. Espíndola, A. Uribe, A. Mendoza and A. Pérez-Vertti, 1999. Distribution of stress and geometry of the Wadati-Benioff zone under Chiapas, Mexico. *Geof. Int., 38*, 95-106.

Rose, W. I., T. J. Bornhorst, S. P. Halsor, W. A. Capaul, S. Lumley, S. De la Cruz-Reyna, M. Mena and R. Mota, 1984. Volcan El Chichón, Mexico: Pre-1982 S-rich eruptive activity. *J. Volcanol. Geotherm. Res., 23*, 147-167.

Rouwet, D., Y. Taran and N. Varley, 2004. Dynamics and mass balance of El Chichón crater lake, Mexico. *Geof. Int., 43*, 427-434.

Rye, R. O., J. F. Luhr and M. D. Wasserman, 1984. Sulfur and oxygen isotopic systematics of the 1982 eruptions of El Chichón Volcano, Chiapas, Mexico, *J. Volcanol. Geotherm. Res., 23*, 109 -123.

Sigurdsson, H., S. N. Carey and J. M. Espíndola, 1984. The 1982 eruptions of El Chichón volcano, Mexico: stratigraphy of pyroclastic deposits. *J. Volcanol. Geotherm. Res., 23,* 11-37.

Sigurdsson, H., S. N. Carey and R. V. Fisher, 1987. The 1982 eruptions of El Chichón volcano, Mexico (3): Physical properties of pyroclastic surges. *Bull. Volcanol., 49*, 467- 488.

Steiger, R. H. and E. Jäger, 1977. Subcommission on geochronology: Convention on the use of decay constants in geo- and cosmochronology: *Earth Planet. Sci. Lett., 36*, 359-362.

Taran, Y., T. P. Fisher, B. Pokrovsky, Y. Sano, M. A. Armienta and J. L. Macías, 1998. Geochemistry of the volcano-hydrothermal system of El Chichón volcano, Chiapas, Mexico. *Bull. Volcanol., 59*, 436-449.

Tassi, F., O. Vaselli, B. Capaccioni, J. L. Macías, A. Nencetti, G. Montegrossi, G. Magro and A. Buccianti, 2003. Chemical composition of fumarolic gases and spring discharges from El Chichón volcano, Mexico: causes and implications of the changes detected over the period 1998-2000. *J. Volcanol. Geotherm. Res., 13*, 105-121.

Tepley lll, F. J., J. P. Davidson, R. I. Tilling and J. G. Arth, 2000. Magma Mixing, Recharge and Eruption Histories Recorded in Plagioclase Phenocrysts from El Chichón Volcano, Mexico, *J. Petrol., 41*, 1397-1411.

Tilling, R. I., M. Rubin, H. Sigurdsson, S. N. Carey, W. A. Duffield and W.I. Rose, 1984. Prehistoric eruptive activity of El Chichón volcano, Mexico. *Science, 224*, 747-749.

Varekamp, J. C., J. F. Luhr and K. L. Prestegaard, 1984. The 1982 eruptions of El Chichón volcano (Chiapas, Mexico): Character of the eruptions, ash-fall deposits, and gas phase. *J. Volcanol. Geotherm. Res., 23*, 39-68.

York, D., C. M. Hall, Y. Yanase, J. A. Hanes and W. J. Kenyon, 1981. $^{40}Ar/^{39}Ar$ dating of terrestrial minerals with a continuous laser. *Geophys. Res. Lett., 8*, 1136-1138.

P. W. Layer[1], A. García-Palomo[2+], D. Jones[1], J. L. Macías[3*], J. L. Arce[2] and J.C. Mora[3]
[1]Geophysical Institute, University of Alaska Fairbanks, Fairbanks, AK, 99775, USA
[2]Departamento de Geología Regional, Instituto de Geología, Universidad Nacional Autónoma de México, Del. Coyoacán 04510, Mexico City, Mexico
[3]Departamento de Vulcanología, Instituto de Geofísica, Universidad Nacional Autónoma de México, Del. Coyoacán 04510, Mexico City, Mexico
**Corresponding author: player@gi.alaska.edu*

Appendix 1. $^{40}Ar/^{39}Ar$ data for whole-rock samples from El Chichon Volcanic Complex.

CHI-017-2 Whole Rock Weighted average of J from standards = 0.0000582 +/- 0.0000002

Laser (mW)	Cum. ^{39}Ar	$^{40}Ar/^{39}Ar$ measured	+/-	$^{37}Ar/^{39}Ar$ measured	+/-	$^{36}Ar/^{39}Ar$ measured	+/-	% Atm. ^{40}Ar	Ca/K	+/-	Cl/K	+/-	$^{40}Ar^*/^{39}ArK$	+/-	Age (ka)	+/- (ka)
700	0.013	9102.825	901.969	0.2899	0.0401	31.1572	3.0902	101.1	0.53	0.07	0.0191	0.0075	-104.14	48.14	-10961	5083
1200	0.051	1710.772	41.341	0.2502	0.0100	5.7644	0.1411	99.6	0.46	0.02	0.0086	0.0012	7.38	8.16	775	856
1600	0.174	128.167	0.358	0.2569	0.0023	0.4256	0.0021	98.1	0.47	0.00	0.0030	0.0002	2.39	0.62	250	65
2000	0.377	13.714	0.118	0.2699	0.0017	0.0434	0.0004	93.5	0.50	0.00	0.0019	0.0001	0.88	0.15	93	16
2500	0.545	6.982	0.050	0.3754	0.0052	0.0214	0.0004	90.6	0.69	0.01	0.0030	0.0001	0.65	0.11	68	11
3000	0.654	7.571	0.077	0.6559	0.0074	0.0219	0.0005	85.3	1.20	0.01	0.0093	0.0003	1.11	0.13	116	13
4500	0.796	8.335	0.049	1.1556	0.0095	0.0237	0.0005	83.4	2.12	0.02	0.0185	0.0002	1.38	0.16	145	17
9000	1.000	13.142	0.065	1.2975	0.0096	0.0309	0.0003	68.9	2.38	0.02	0.0148	0.0001	4.09	0.09	429	10
Integrated		206.271	0.581	0.6633	0.0028	0.6958	0.0028	99.7	1.22	0.01	0.0085	0.0001	0.68	0.68	72	72

CHI-0804-01 Whole Rock Weighted average of J from standards = 0.0000582 +/- 0.0000002

Laser (mW)	Cum. ^{39}Ar	$^{40}Ar/^{39}Ar$ measured	+/-	$^{37}Ar/^{39}Ar$ measured	+/-	$^{36}Ar/^{39}Ar$ measured	+/-	% Atm. ^{40}Ar	Ca/K	+/-	Cl/K	+/-	$^{40}Ar^*/^{39}ArK$	+/-	Age (ka)	+/- (ka)
700	0.018	162.052	1.760	0.5502	0.0092	0.5396	0.0081	98.4	1.01	0.02	0.0036	0.0005	2.62	1.74	275	183
1200	0.174	13.192	0.064	0.2806	0.0022	0.0442	0.0006	99.0	0.51	0.00	0.0007	0.0001	0.13	0.16	14	16
1600	0.528	2.756	0.016	0.2949	0.0022	0.0089	0.0002	95.8	0.54	0.00	0.0005	0.0000	0.12	0.05	12	5
2000	0.738	6.263	0.042	0.4338	0.0030	0.0217	0.0003	102.2	0.80	0.01	0.0007	0.0000	-0.13	0.09	-14	9
2500	0.829	26.759	0.169	0.9302	0.0071	0.0925	0.0009	102.0	1.71	0.01	0.0065	0.0002	-0.54	0.25	-57	26
3000	0.893	42.884	0.371	1.6342	0.0184	0.1408	0.0022	96.8	3.00	0.03	0.0177	0.0003	1.37	0.58	144	61
4000	0.954	41.233	0.214	2.9693	0.0202	0.1357	0.0012	96.8	5.46	0.04	0.0328	0.0003	1.33	0.35	140	37
6000	0.988	58.911	0.361	5.2153	0.0354	0.1736	0.0021	86.5	9.60	0.07	0.0343	0.0005	7.99	0.59	839	62
9000	1.000	107.706	1.006	5.2014	0.0644	0.3212	0.0052	87.8	9.58	0.12	0.0267	0.0007	13.19	1.33	1384	140
Integrated		18.311	0.048	0.8616	0.0027	0.0600	0.0003	96.5	1.58	0.01	0.0057	0.0000	0.63	0.07	66	8

CHI-0804-04 Whole Rock Weighted average of J from standards = 0.0000582 +/- 0.0000002

Laser (mW)	Cum. ^{39}Ar	$^{40}Ar/^{39}Ar$ measured	+/-	$^{37}Ar/^{39}Ar$ measured	+/-	$^{36}Ar/^{39}Ar$ measured	+/-	% Atm. ^{40}Ar	Ca/K	+/-	Cl/K	+/-	$^{40}Ar^*/^{39}ArK$	+/-	Age (ka)	+/- (ka)
700	0.055	5.517	0.087	0.2617	0.0076	0.0198	0.0016	106.3	0.48	0.01	0.0064	0.0004	-0.35	0.48	-37	50
1200	0.256	1.250	0.020	0.3144	0.0034	0.0043	0.0005	102.5	0.58	0.01	0.0040	0.0001	-0.03	0.15	-3	16
1600	0.424	0.700	0.019	0.1774	0.0058	0.0028	0.0007	121.8	0.33	0.01	0.0042	0.0002	-0.15	0.22	-15	23
2000	0.560	0.567	0.023	0.2184	0.0061	0.0031	0.0006	166.4	0.40	0.01	0.0053	0.0001	-0.36	0.19	-38	20
2500	0.678	0.629	0.024	0.2604	0.0055	0.0023	0.0007	111.8	0.48	0.01	0.0070	0.0002	-0.07	0.20	-7	21
3000	0.765	1.566	0.072	0.4716	0.0055	0.0042	0.0010	77.7	0.87	0.01	0.0093	0.0003	0.34	0.30	36	31
4000	0.883	4.025	0.052	0.7308	0.0094	0.0123	0.0008	89.8	1.34	0.02	0.0137	0.0004	0.41	0.23	43	24
6000	0.985	9.698	0.073	2.0946	0.0146	0.0212	0.0016	63.3	3.85	0.03	0.0272	0.0004	3.56	0.47	373	50
9000	1.000	21.935	0.428	4.1075	0.0956	0.0583	0.0145	77.2	7.56	0.18	0.0429	0.0020	5.00	4.29	525	450
Integrated		2.762	0.014	0.5717	0.0027	0.0080	0.0004	85.0	1.05	0.00	0.0092	0.0001	0.41	0.11	43	12

CHI-0804-08A Whole Rock Weighted average of J from standards = 0.0000582 +/- 0.0000002

Laser (mW)	Cum. ^{39}Ar	$^{40}Ar/^{39}Ar$ measured	+/-	$^{37}Ar/^{39}Ar$ measured	+/-	$^{36}Ar/^{39}Ar$ measured	+/-	% Atm. ^{40}Ar	Ca/K	+/-	Cl/K	+/-	$^{40}Ar^*/^{39}ArK$	+/-	Age (ka)	+/- (ka)
700	0.112	649.115	4.240	2.3383	0.0297	2.1921	0.0161	99.8	4.30	0.05	0.0548	0.0014	1.51	3.78	159	397
1200	0.266	58.702	0.588	3.0415	0.0295	0.1816	0.0025	91.1	5.59	0.05	0.0521	0.0007	5.25	0.60	551	63
1600	0.382	27.754	0.292	1.3575	0.0199	0.0803	0.0034	85.2	2.49	0.04	0.0496	0.0012	4.10	0.99	430	104
2000	0.482	19.023	0.268	1.1349	0.0487	0.0536	0.0042	83.0	2.08	0.09	0.0496	0.0017	3.23	1.24	339	130
2500	0.592	15.254	0.220	1.6440	0.0397	0.0368	0.0045	70.6	3.02	0.07	0.0539	0.0016	4.48	1.34	470	141
3000	0.700	19.004	0.232	1.3870	0.0300	0.0517	0.0030	80.0	2.55	0.06	0.0590	0.0014	3.80	0.89	398	93
4000	0.848	16.349	0.217	1.5112	0.0318	0.0481	0.0044	86.3	2.78	0.06	0.0554	0.0009	2.23	1.29	234	136
6000	0.978	16.520	0.141	1.9326	0.0504	0.0435	0.0036	77.1	3.55	0.09	0.0583	0.0029	3.78	1.05	396	110
9000	1.000	45.534	1.543	2.3120	0.1047	0.1302	0.0210	84.2	4.25	0.19	0.0423	0.0024	7.21	6.16	756	646
Integrated		96.340	0.384	1.8578	0.0125	0.3140	0.0020	96.2	3.41	0.02	0.0539	0.0005	3.66	0.57	384	60

CHI-0804-08B Whole Rock Weighted average of J from standards = 0.0000582 +/- 0.0000002

Laser (mW)	Cum. ^{39}Ar	^{40}Ar/^{39}Ar measured	+/-	^{37}Ar/^{39}Ar measured	+/-	^{36}Ar/^{39}Ar measured	+/-	% Atm. 40Ar	Ca/K	+/-	Cl/K	+/-	^{40}Ar*/^{39}ArK	+/-	Age (ka)	+/- (ka)
600	0.044	214.425	1.328	0.3805	0.0109	0.7035	0.0055	96.9	0.70	0.02	0.0084	0.0006	6.55	1.55	687	162
1200	0.200	32.936	0.147	0.3886	0.0068	0.1087	0.0012	97.5	0.71	0.01	0.0031	0.0001	0.81	0.37	85	38
1800	0.319	6.494	0.048	0.4293	0.0040	0.0198	0.0007	89.9	0.79	0.01	0.0042	0.0001	0.66	0.20	69	21
2400	0.448	5.509	0.038	0.5432	0.0051	0.0172	0.0007	91.8	1.00	0.01	0.0090	0.0002	0.45	0.20	47	21
3000	0.565	6.053	0.051	0.6485	0.0108	0.0186	0.0003	90.3	1.19	0.02	0.0112	0.0002	0.58	0.09	61	9
4500	0.814	6.656	0.049	0.8666	0.0078	0.0190	0.0003	83.7	1.59	0.01	0.0117	0.0002	1.08	0.10	114	10
9000	1.000	8.282	0.078	1.0280	0.0103	0.0178	0.0004	62.6	1.89	0.02	0.0177	0.0003	3.09	0.12	324	13
Integrated		19.932	0.067	0.6815	0.0031	0.0626	0.0004	92.7	1.25	0.01	0.0100	0.0001	1.46	0.10	154	11

CHI-9320 Whole Rock Weighted average of J from standards = 0.0000582 +/- 0.0000002

Laser (mW)	Cum. ^{39}Ar	^{40}Ar/^{39}Ar measured	+/-	^{37}Ar/^{39}Ar measured	+/-	^{36}Ar/^{39}Ar measured	+/-	% Atm. 40Ar	Ca/K	+/-	Cl/K	+/-	^{40}Ar*/^{39}ArK	+/-	Age (ka)	+/- (ka)
600	0.087	6.490	0.058	0.1126	0.0025	0.0217	0.0006	99.0	0.21	0.00	0.0013	0.0001	0.06	0.18	7	19
1200	0.371	1.120	0.009	0.0894	0.0014	0.0036	0.0002	97.7	0.16	0.00	0.0008	0.0001	0.03	0.06	3	7
1800	0.651	1.663	0.011	0.0827	0.0011	0.0055	0.0002	99.3	0.15	0.00	0.0014	0.0001	0.01	0.07	1	7
2400	0.837	3.783	0.022	0.1173	0.0012	0.0124	0.0003	97.4	0.22	0.00	0.0029	0.0001	0.10	0.08	10	9
3000	0.901	4.520	0.027	0.1500	0.0038	0.0167	0.0008	109.4	0.28	0.01	0.0034	0.0002	-0.42	0.23	-45	24
4500	0.957	5.140	0.038	0.2053	0.0041	0.0178	0.0010	102.4	0.38	0.01	0.0043	0.0002	-0.12	0.30	-13	32
9000	1.000	6.150	0.084	0.2239	0.0087	0.0186	0.0009	89.6	0.41	0.02	0.0052	0.0004	0.64	0.28	67	29
Integrated		2.896	0.010	0.1109	0.0008	0.0096	0.0002	99.1	0.20	0.00	0.0020	0.0000	0.03	0.04	3	4

CHI-9323 Whole Rock Weighted average of J from standards = 0.0000582 +/- 0.0000002

Laser (mW)	Cum. ^{39}Ar	^{40}Ar/^{39}Ar measured	+/-	^{37}Ar/^{39}Ar measured	+/-	^{36}Ar/^{39}Ar measured	+/-	% Atm. ^{40}Ar	Ca/K	+/-	Cl/K	+/-	^{40}Ar*/^{39}ArK	+/-	Age (ka)	+/- (ka)
600	0.125	1148.390	10.170	0.0573	0.0023	3.5339	0.0358	90.9	0.11	0.00	0.0033	0.0010	104.11	7.17	10892	748
1200	0.446	405.850	1.395	0.0854	0.0009	1.2538	0.0067	91.3	0.16	0.00	0.0022	0.0005	35.34	2.31	3705	242
1800	0.653	551.755	1.935	0.1421	0.0020	1.7226	0.0077	92.3	0.26	0.00	0.0030	0.0005	42.70	2.78	4475	291
2400	0.762	861.765	6.452	0.2306	0.0040	2.6932	0.0220	92.4	0.42	0.01	0.0050	0.0008	65.93	4.59	6905	480
3000	0.829	1396.841	15.740	0.3074	0.0081	4.3495	0.0522	92.0	0.56	0.01	0.0100	0.0012	111.60	8.11	11672	846
4500	0.929	2096.923	38.790	0.5076	0.0096	6.4370	0.1210	90.7	0.93	0.02	0.0178	0.0030	194.87	11.62	20334	1206
9000	1.000	2704.359	70.375	1.0176	0.0276	8.1852	0.2174	89.4	1.87	0.05	0.0471	0.0028	285.86	18.82	29750	1942
Integrated		976.758	3.187	0.2326	0.0013	3.0091	0.0110	91.0	0.43	0.00	0.0081	0.0004	87.57	2.24	9166	236

CHI-9331 Whole Rock Weighted average of J from standards = 0.0000582 +/- 0.0000002

Laser (mW)	Cum. ^{39}Ar	^{40}Ar/^{39}Ar measured	+/-	^{37}Ar/^{39}Ar measured	+/-	^{36}Ar/^{39}Ar measured	+/-	% Atm. ^{40}Ar	Ca/K	+/-	Cl/K	+/-	^{40}Ar*/^{39}ArK	+/-	Age (ka)	+/- (ka)
600	0.057	47.280	0.272	0.4590	0.0109	0.1477	0.0018	92.3	0.84	0.02	0.0051	0.0004	3.63	0.49	381	51
1200	0.268	6.563	0.044	0.4229	0.0047	0.0151	0.0005	67.6	0.78	0.01	0.0020	0.0001	2.12	0.16	222	16
1800	0.533	5.565	0.033	0.4665	0.0092	0.0121	0.0004	64.1	0.86	0.02	0.0031	0.0001	1.99	0.11	208	12
2400	0.740	4.999	0.043	0.6285	0.0080	0.0095	0.0003	55.3	1.15	0.01	0.0075	0.0002	2.22	0.09	233	10
3000	0.882	6.458	0.041	0.8585	0.0061	0.0139	0.0004	62.7	1.58	0.01	0.0127	0.0003	2.40	0.12	252	12
4500	0.964	6.781	0.070	0.8966	0.0117	0.0155	0.0012	66.6	1.65	0.02	0.0130	0.0003	2.25	0.34	237	35
9000	1.000	7.816	0.100	0.9424	0.0177	0.0188	0.0014	70.5	1.73	0.03	0.0134	0.0004	2.30	0.42	241	44
Integrated		8.334	0.026	0.5984	0.0035	0.0207	0.0002	72.9	1.10	0.01	0.0064	0.0001	2.25	0.07	236	7

CHI-9364 Whole Rock #1 Weighted average of J from standards = 0.0000582 +/- 0.0000002

Laser (mW)	Cum. ^{39}Ar	^{40}Ar/^{39}Ar measured	+/-	^{37}Ar/^{39}Ar measured	+/-	^{36}Ar/^{39}Ar measured	+/-	% Atm. ^{40}Ar	Ca/K	+/-	Cl/K	+/-	^{40}Ar*/^{39}ArK	+/-	Age (ka)	+/- (ka)
600	0.005	2550.305	65.692	1.2316	0.0764	8.5295	0.2248	98.8	2.26	0.14	0.0386	0.0036	29.92	16.71	3137	1750
1200	0.006	955.160	68.140	0.8740	0.2315	3.1738	0.2340	98.2	1.60	0.43	0.0043	0.0083	17.35	18.94	1819	1985
1800	0.007	640.410	60.287	0.6020	0.3834	2.3719	0.2664	109.4	1.11	0.70	-0.0028	0.0116	-60.48	43.74	-6358	4606
2400	0.007	1218.950	384.019	-0.5685	1.3882	3.8253	1.2518	92.7	-1.04	2.55	-0.0181	0.0378	88.48	104.39	9261	10898
3000	0.007	1235.288	444.199	4.2830	2.0850	4.1743	1.5388	99.8	7.88	3.85	-0.0223	0.0464	2.08	101.00	218	10597
4500	0.675	70.151	0.263	0.6435	0.0029	0.2315	0.0013	97.5	1.18	0.01	0.0045	0.0001	1.76	0.36	185	38
9000	1.000	13.008	0.078	0.4353	0.0039	0.0402	0.0004	91.3	0.80	0.01	0.0104	0.0001	1.12	0.10	118	11
Integrated		65.876	0.207	0.5794	0.0024	0.2173	0.0010	97.4	1.06	0.00	0.0066	0.0001	1.69	0.26	178	27

CHI-9364 Whole Rock #2 Weighted average of J from standards = 0.0000582 +/- 0.0000002

Laser (mW)	Cum. ^{39}Ar	^{40}Ar/39Ar measured	+/-	^{37}Ar/^{39}Ar measured	+/-	^{36}Ar/^{39}Ar measured	+/-	% Atm. ^{40}Ar	Ca/K	+/-	Cl/K	+/-	^{40}Ar*/^{39}ArK	+/-	Age (ka)	+/- (ka)
600	0.018	1569.293	34.995	0.7521	0.0456	5.2191	0.1182	98.3	1.38	0.08	0.0242	0.0019	27.10	7.27	2842	762
1200	0.070	273.846	1.848	1.2712	0.0213	0.9006	0.0084	97.2	2.33	0.04	0.0065	0.0005	7.79	2.17	817	228
1800	0.162	47.157	0.290	1.1672	0.0110	0.1546	0.0017	96.7	2.14	0.02	0.0020	0.0002	1.54	0.42	161	44
2400	0.282	28.477	0.153	0.8681	0.0090	0.0903	0.0017	93.5	1.59	0.02	0.0024	0.0002	1.85	0.49	194	51
3000	0.471	16.123	0.084	0.4182	0.0037	0.0522	0.0007	95.7	0.77	0.01	0.0029	0.0002	0.69	0.21	73	22
4500	0.770	12.083	0.071	0.3221	0.0023	0.0379	0.0005	92.7	0.59	0.00	0.0063	0.0001	0.87	0.16	92	17
9000	1.000	13.247	0.117	0.5403	0.0057	0.0402	0.0005	89.5	0.99	0.01	0.0142	0.0002	1.39	0.13	146	13
Integrated		59.972	0.164	0.5907	0.0026	0.1964	0.0008	96.7	1.08	0.00	0.0069	0.0001	1.97	0.20	207	21

CHI-9521 Whole Rock #1 Weighted average of J from standards = 0.0000853 +/- 0.0000002

Laser (mW)	Cum. ^{39}Ar	^{40}Ar/^{39}Ar measured	+/-	^{37}Ar/^{39}Ar measured	+/-	^{36}Ar/^{39}Ar measured	+/-	% Atm. ^{40}Ar	Ca/K	+/-	Cl/K	+/-	^{40}Ar*/^{39}ArK	+/-	Age (ka)	+/- (ka)
300	0.013	343.309	3.611	0.1910	0.0141	1.1683	0.0135	100.6	0.35	0.03	0.0060	0.0008	-1.95	2.44	-300	376
600	0.078	50.574	0.297	0.2101	0.0036	0.1699	0.0015	99.3	0.39	0.01	0.0043	0.0002	0.36	0.41	55	64
1000	0.247	15.377	0.097	0.2362	0.0028	0.0526	0.0005	101.1	0.43	0.01	0.0021	0.0001	-0.17	0.14	-26	21
1500	0.431	13.094	0.078	0.2866	0.0028	0.0455	0.0007	102.7	0.53	0.01	0.0018	0.0001	-0.35	0.19	-54	30
2000	0.566	19.583	0.083	0.3993	0.0040	0.0660	0.0006	99.5	0.73	0.01	0.0021	0.0001	0.09	0.16	14	25
2000	0.616	33.512	0.193	0.4674	0.0085	0.1141	0.0023	100.6	0.86	0.02	0.0024	0.0002	-0.21	0.66	-32	102
2700	0.685	68.463	0.397	0.6490	0.0076	0.2357	0.0022	101.7	1.19	0.01	0.0052	0.0002	-1.16	0.64	-179	98
3400	0.782	145.301	0.624	1.0431	0.0083	0.5054	0.0041	102.8	1.92	0.02	0.0131	0.0003	-4.00	1.10	-616	170
5200	0.928	167.522	0.595	2.2370	0.0118	0.5701	0.0033	100.5	4.11	0.02	0.0360	0.0003	-0.81	0.88	-124	135
6000	0.969	283.611	1.423	1.6894	0.0220	0.9570	0.0067	99.7	3.10	0.04	0.0248	0.0006	0.91	1.53	140	235
9000	1.000	310.713	1.699	1.8212	0.0150	1.0320	0.0091	98.1	3.35	0.03	0.0184	0.0006	5.88	2.24	905	345
Integrated		81.754	0.144	0.7849	0.0024	0.2783	0.0008	100.6	1.44	0.00	0.0099	0.0001	-0.46	0.21	-70	32

CHI-9521 Whole Rock #2 Weighted average of J from standards = 0.0000853 +/- 0.0000002

Laser (mW)	Cum. ^{39}Ar	^{40}Ar/^{39}Ar measured	+/-	^{37}Ar/^{39}Ar measured	+/-	^{36}Ar/^{39}Ar measured	+/-	% Atm. ^{40}Ar	Ca/K	+/-	Cl/K	+/-	^{40}Ar*/^{39}ArK	+/-	Age (ka)	+/- (ka)
300	0.018	144.780	1.512	0.1954	0.0101	0.4949	0.0076	101.0	0.36	0.02	0.0057	0.0007	-1.48	1.73	-227	267
600	0.103	33.288	0.121	0.1994	0.0027	0.1123	0.0012	99.7	0.37	0.00	0.0035	0.0002	0.09	0.36	14	55
1000	0.304	11.749	0.063	0.2299	0.0022	0.0406	0.0005	102.1	0.42	0.00	0.0015	0.0001	-0.24	0.15	-37	23
1500	0.496	11.821	0.075	0.3005	0.0035	0.0396	0.0005	98.9	0.55	0.01	0.0014	0.0001	0.13	0.13	19	21
2000	0.607	20.792	0.107	0.4502	0.0051	0.0713	0.0009	101.3	0.83	0.01	0.0022	0.0001	-0.28	0.25	-43	39
2700	0.694	64.003	0.439	0.7431	0.0094	0.2203	0.0022	101.7	1.36	0.02	0.0066	0.0002	-1.06	0.57	-163	87
3400	0.786	141.893	0.628	1.1856	0.0104	0.4910	0.0035	102.2	2.18	0.02	0.0154	0.0003	-3.12	0.88	-481	135
5200	0.912	159.268	0.625	2.2355	0.0133	0.5395	0.0036	100.0	4.11	0.02	0.0332	0.0004	-0.01	0.93	-1	143
6000	0.959	255.876	1.601	1.7874	0.0160	0.8558	0.0065	98.8	3.28	0.03	0.0223	0.0006	3.11	1.20	478	184
7000	0.981	261.140	2.002	1.6523	0.0173	0.8687	0.0106	98.3	3.04	0.03	0.0208	0.0007	4.53	2.91	697	447
9000	1.000	258.235	2.589	1.8306	0.0218	0.8646	0.0105	98.9	3.36	0.04	0.0185	0.0009	2.85	2.26	439	348
Integrated		73.772	0.141	0.7855	0.0025	0.2503	0.0008	100.2	1.44	0.00	0.0092	0.0001	-0.15	0.19	-24	29

CHI-95HOST Whole Rock Weighted average of J from standards = 0.0000582 +/- 0.0000002

Laser (mW)	Cum. ^{39}Ar	^{40}Ar/^{39}Ar measured	+/-	^{37}Ar/^{39}Ar measured	+/-	^{36}Ar/^{39}Ar measured	+/-	% Atm. ^{40}Ar	Ca/K	+/-	Cl/K	+/-	^{40}Ar*/^{39}ArK	+/-	Age (ka)	+/- (ka)
600	0.049	42.697	0.260	0.2570	0.0167	0.1405	0.0020	97.2	0.47	0.03	0.0614	0.0007	1.19	0.60	124	63
1200	0.295	4.801	0.032	0.2635	0.0039	0.0153	0.0004	94.4	0.48	0.01	0.0448	0.0004	0.27	0.13	28	13
1800	0.596	5.197	0.028	0.3532	0.0054	0.0163	0.0004	92.6	0.65	0.01	0.0306	0.0004	0.38	0.10	40	11
2400	0.750	12.621	0.062	0.6222	0.0066	0.0426	0.0004	99.6	1.14	0.01	0.0312	0.0003	0.05	0.12	5	13
3000	0.842	23.120	0.172	0.9108	0.0150	0.0778	0.0015	99.3	1.67	0.03	0.0400	0.0006	0.16	0.42	17	44
4500	0.950	30.692	0.152	1.3272	0.0157	0.0966	0.0009	92.8	2.44	0.03	0.0441	0.0005	2.22	0.26	233	28
9000	1.000	39.468	0.265	2.0756	0.0198	0.1054	0.0020	78.5	3.81	0.04	0.0449	0.0005	8.47	0.57	889	60
Integrated		14.181	0.037	0.6105	0.0034	0.0449	0.0003	93.5	1.12	0.01	0.0387	0.0002	0.92	0.08	97	8

CHI-SOMMA Whole Rock Weighted average of J from standards = 8.349e-05 2.946e-07

Laser (mW)	Cum. ^{39}Ar	$^{40}Ar/^{39}Ar$ measured	+/-	$^{37}Ar/^{39}Ar$ measured	+/-	$^{36}Ar/^{39}Ar$ measured	+/-	% Atm. ^{40}Ar	Ca/K	+/-	Cl/K	+/-	$^{40}Ar^*/^{39}ArK$	+/-	Age (ka)	+/- (ka)
500	0.009	170.297	1.224	0.3466	0.0087	0.5749	0.0056	99.8	0.64	0.02	0.0030	0.0010	0.40	1.46	60	220
900	0.051	13.235	0.077	0.2725	0.0029	0.0452	0.0008	100.9	0.50	0.01	0.0013	0.0002	-0.11	0.22	-17	34
1300	0.142	3.866	0.028	0.2104	0.0024	0.0131	0.0003	100.8	0.39	0.00	0.0010	0.0001	-0.03	0.10	-4	15
1700	0.263	1.771	0.017	0.1947	0.0027	0.0061	0.0003	102.5	0.36	0.00	0.0011	0.0001	-0.04	0.07	-7	11
2100	0.396	1.406	0.014	0.2001	0.0016	0.0049	0.0002	104.5	0.37	0.00	0.0015	0.0001	-0.06	0.06	-9	9
2500	0.514	1.754	0.016	0.2199	0.0022	0.0061	0.0004	103.0	0.40	0.00	0.0020	0.0001	-0.05	0.10	-8	16
3000	0.617	2.931	0.025	0.2475	0.0027	0.0106	0.0003	107.7	0.45	0.00	0.0028	0.0001	-0.22	0.10	-34	15
4000	0.751	10.709	0.087	0.3295	0.0030	0.0367	0.0006	101.4	0.60	0.01	0.0051	0.0001	-0.15	0.17	-22	26
6000	0.944	15.705	0.110	0.7373	0.0053	0.0525	0.0004	98.6	1.35	0.01	0.0112	0.0001	0.21	0.12	32	19
Integrated		9.690	0.027	0.4482	0.0014	0.0322	0.0002	98.1	0.82	0.00	0.0052	0.0000	0.18	0.05	28	7